Response to reviewers

Reviewer comments are in normal text, and our responses are in bold

Comments from Gianvito Scaringi

Dear authors,
I enjoyed reading your manuscript, which I believe can be a useful contribution towards landslide risk reduction in highly seismic regions. I have a few questions, mostly regarding the robustness of your findings, which I list as follows:
- You mentioned multiple times that the DEM resolution can influence some of your results. It would be nice to quantify this influence at least for one inventory for which a higher resolution DEM is available (e.g. Northridge). Perhaps, moving from 30 m to 10 m DEM will only produce marginal improvements while increasing the computational cost significantly, or on the contrary it will change the result significantly.

We have tested the impact of varying DEM resolution from 10 – 90 m for the Northridge study area. We find that performance of slope, skyline angle and upslope contributing area improves slightly at finer resolutions. Hazard area preforms best at the same resolution as that used for parameter optimization (in this case 30 m). Nevertheless, we find that the hazard area metric remains the most skillful predictor of hazard across grid resolutions from 10 m to 60 m, and thus that the rule even when applied over length scales as small as 10 m or as large as 60 m will continue to perform 'well' relative to the alternatives. A description of this test has been added to the Discussion.

- There are cases in which several inventories are available for the same study area (e.g. Wenchuan). These inventories are sometimes quite different from each other. Among others, we discussed this in a recent submission, still under review (see the revised manuscript in the discussion at https://www.earth-syst-sci-data-discuss.net/essd-2018-105/) and we found substantial areal mismatches (up to 67%) between inventories in the Wenchuan, and rather low pixel-based correlations (R-squared as low as 0.35). We showed that this translates in quite some differences in landslide-size probability distributions and hence in landslide volume estimations. This might condition some types of hazard assessments based on volume-runout correlations. However, we did not go deeper into the topic, as it was out of the scope of our manuscript, and we did not investigate how this mismatch between inventories translates into statistics of controlling factors (e.g. slope, upstream contributing area, etc.). It would be interesting if you could estimate to what extent choosing a different inventory for the same study area would affect your assessment.

We have tested the impact of different landslide inventories for the Wenchuan earthquake and now report the results in the discussion. We find that the change of inventory has no impact on the rank order of performance of the metrics; and a very minor impact on both the AUC values and the hazard curves. As above, we now provide a description of this test in the Discussion

- Also, again about the Wenchuan case, you only chose a subset of the inventory by Li et al. (2014) containing about 1/3 of the landslides. It would be good to explain whether this subset can be thought as representative of the entire study area (e.g. in terms of landslide metrics, topography, lithology, distance from epicentre and fault rupture, etc.) so that one would be confident that the results you obtain have more general validity and are not biased by your choice, which was only due to a data availability issue. What you report in the conclusion (see my point below), that is that the site-specific and averaged rules perform similarly, is comforting in this sense, but what if it is just a coincidence?

Subsetting was necessary because gaps in the SRTM would result in incorrect computations for our topographic metrics, particularly upslope contributing area and hazard area. The subset of landslides that we use run in a swath from north to south. The area extends from the footwall to the hanging wall of the fault crossing the surface expression of the fault and thus spans almost the full range of shaking intensities, lithologies, and topographic settings. Thus, while we cannot rule out the possibility that the site-specific rule for Wenchuan would be different with the full data set, we see no reason why that should be the case. The fact that site-specific and averaged values for hazard area are essentially equivalent also suggests that we are looking at general patterns rather than coincidental relationships. We now include a series of study area maps in the supplementary information showing the study areas and the mapped landslides superimposed on the DEMs. For Wenchuan we show both the full set of landslides mapped by Li et al. (2014) and the subset that we use.

- From your analyses you obtained a set of simple and easily understandable rules to minimise the exposure, and you wrote that the hazard area calculated with averaged parameters performs only slightly worse than hazard area calculated with site-specific parameters. This is encouraging and, as you wrote, it suggests that the average parameters can be applied to other inventories (or subsets of inventories). Thus, it would be very interesting to see these averaged parameters being applied to other inventories, across a variety of landscapes, climates and seismic characteristics. Also, it would be interesting to apply your rules to a highly seismic region in which no recent earthquake has occurred, and relate it to the current distribution of population and exposed goods (but I recognise the latter is out of the scope of this work, so it is just an idea).

These are both very interesting ideas, though we feel that they are out of scope for this work as you say. We are keen to examine these rules in different contexts to establish the range of conditions under which they apply, but felt that the six cases used here make a useful initial contribution. We have taken an approach similar to your second idea to provide an indication of the spatial distribution of co-seismic landslides that might be expected in a scenario earthquake for the specific case of an earthquake on the Weinan-Jinyang fault near Xian, China (covered in a separate manuscript submitted to IJDRR).

Reviewer 1: Odin Marc

Summary

Milledge et al., present a thorough statistical analysis of six coseismic landslides inventories to relate landslide hazard to landscape properties such as slope and contributing areas, but also more specific variables such as skyline angle and a hazard area integrating the probability of initiation and propagation of landslides. They found that the two latter metrics explain best the location of the inventories and may allow to be converted into simple rules useful for hazard management. The paper is well written, with a straight forward structure and informative. It will make a nice contribution for NHESS both for its systematic analysis and its recommendations. I have two major comments that I think could improve the results and the discussion, and then give a number of minor Line by Line comments with potential clarification or additional small analysis.

Major Comments

My first comment is about the normalization of several of the hazard metrics : I am convinced that a substantial part of the difference between the hazard curves could be removed by plotting the hazard against a landscape metric : For example for slope, each landscape as likely a modal slope, that may be interpreted as the result of geolechanical difference (for steady state landscape at least). Thus curves may be plotted against S-mode(S) , somewhat normalizing for difference between two landscape. I can understand the author may still want to express their rules in terms of absolute values of slope or other variables, but I suspect this normalization would clarify and strengthen the result and their analysis (as this did in other studies). I make suggestion for the other variables in my inline comments.

This is an excellent suggestion, and indeed we found that normalization collapses the hazard curves to some extent. This is very satisfying in terms of explaining our observations. We include these new results in our revised manuscript though they do not alter our conclusions since normalization does not alter the rank order or improve predictive skill of any metric.

My second concern is that their maybe some over-interpretation of the data scatter towards the extremity of the hazard curves. And the author do not provide clear metrics or indication of the validity of individual datapoint. This is not an easy task but the work of Rault et al., which I co-authored, recently proposed a method to do exactly that. I would suggest the author to apply these criterium and check.
In this work we consider: the probabilty p of the whole topography, and the one resulting from the landslides affected area only p_L.
To assess whether p_L is significantly different from p we compute the confidence interval Ip associated to the random drawing of n (n the number of landslides) pixels out of the landscape distribution. If p_L belongs to [p-Ip : p+Ip] then we cannot exclude that the difference between p and p_L just comes from random fluctuations and it is likely not significant. Given landslides remain rare in the whole topography, the drawing can be assumed independent, and similar to a Bernoulli sampling. Provided the central limit theorem is respected (i.e. n>30, np>5 and n(1-p)>5) the 90% confidence interval can be estimated as:

Ip = p – 1.96 (p(1-p)/n)^0.5 ; p + 1.96 (p(1-p)/n)^0.5. Some additional details can be found in the supplementary methods of Rault et al., 2018. Basically n is large (n>1000-10,000) so the authors should obtain very narrow Ip until they reach p<0.001 – 0.0001 but I expect these low probability to be reached in the tail of the distribution (Fig 3,4, 6) and the cut off will vary for the different landscape with higher or lower p or n. The authors could compute Ip as well as the convergence criterium and show the points which may be insignificant in shaded / transparent ?

Thank you for pointing us to this approach. We had struggled to find a way to account for sample sizes in our analysis but the Rault et al. approach is extremely well suited to the problem! We have now implemented this method in all cases where we generate hazard curves (i.e. conditional probability curves). In each case (Figs 3-5) we show both those data points that show a significant difference and those that don't, and we explain this distinction in the text.

<u>Line By line comments:</u>
L123 : I could not find Milledge 2018 in the reference list... please check. **Added.**

L133: Add couple of reference for shaking: e.g. Khazai and Sitar 2004, Meunier 2007. **Added on L141**

L138: I think you should also cite Meunier 2008 here, and probably the recent analysis discussion for an extended number of earthquakes in Rault et al., 2018. **Added on L145.**

L142:152 : A couple of references on the suspected effects would be relevant. Especially the ones cited elsewhere in the text: Parise and Jibson 2000, for lithology, Maufroy et al., 2015 for curvature and ridge amplification. **Added on L154-159.**

L155: True they pertain to initiation, but vast majority of studies highlighting their role or quantifying statistical relations between these predictors and landslide use total area and therefore are combining both initiation and runout.
We agree. However, the mechanistic justification for the factors is almost always initiation based, as are the GIS approaches that are typically applied to assess landslide susceptibility. Our point here is that when these variables are used for landslide hazard prediction they are used to represent controls on landslide initiation. We have modified the sentence to say:
"The potential predictors described above are primarily chosen in hazard models for their perceived link to the probability of coseismic landslide initiation." (L163).

L180: I have the impression it should be the minimum skyline angle, not intersecting topography, …. Indeed a maximum reach angle. Cf comment on Fig 1
We could phrase this either as: 'the maximum angle from horizontal to the skyline' or 'the minimum angle from the horizontal that does not intersect the skyline'. We have chosen the former because it is shorter and because we are concerned that the latter is more open to misinterpretation. In particular, people may not think of cones at increasing angles and thus may misunderstand or ignore the second clause.

L200 – 300: This is certainly at the appreciation of the authors, but I have the impression the earthquake environment (tectonic, climatic, vegetation) is over described. Given you never re-refer to this context later, you may shrink those description and end this section with a sentence like : "these epicentral areas encompasses a large diversity of tectonic (X to Z) , climatic (X to Y) and vegetation cover (X to Y) contexts, but we assume landslides in all of them should be at first order driven by topographic parameters in the same way".
Thank you, this is a useful suggestion. We have considerably shortened this section, compressed the information into a table in the Supplementary Information, and added a summary paragraph in line with your suggestion.

In contrast, some aspects may be missing or insufficiently discussed:
1/ I think the number of landslide polygons used in Chi-Chi is missing. **Agreed, added on L229**
2/ The fact you used a sub-inventories in Wenchuan may mean you artificially limit your analysis to a range of shaking quite different from the other cases . This should be mentionned.
We agree that this is an important issue and needs clarifying, as also mentioned in our response to Dr Scaringi's comments above. We have added maps of the study areas in the Supplementary Information to help readers interpret our results. In the Wenchuan case we show both the full

inventory of Li et al. (2014) and the subset that we use. We have added a statement in the paper itself (L239-242) to show that the range of PGA values experienced in our Wenchuan study area (0.16-1.3 g) is similar to those for the whole inventory (0.12-1.3 g).

3/ A few words on the Implications of polygon mapping quality on your analysis may be given here (or in discussion), such as the affect of amalgamation ; inclusion or not of debris flow propagation within the river network ? (I know it is a difficult distinction, often ignored but it should impact the statistics, especially of contributing area for example). Implictions of the different resolution limit (for Chi Chi or FInisterre compared to Northridge) or of the location accuracy ?
Agreed, we have now added a paragraph on mapping quality in the discussion (L840-853)

Figure 1: Caption: a cone projected from P no ? **Agreed, modified.**
If your cone as angle define from horizontal upward, are you looking for the minimum skyline angle, not intersecting the topography? That is what I get from your sketch in c). See previous comment about skyline angle definition.
Both are possible definitions of the angle we are seeking, but we believe our current definition is less open to misinterpretation (see response to comment on line 180 above).

L372-380: < 10 observations ? Why ? And this is only for the 2 ariable case (Fig 4). For the single variable case it is not clear what is noisy data and where to really set the boundary or unsignificant datapoints. Rault et al., 2018 propose an extension of Meunier et al., 2008 studies with an estimation of the uncertainty of observations based on both the number of observations and the probability. See major comments.
We have now applied the Rault et al approach, so thank you for pointing it out to us.

L458: Shalrun-EQ= Probability of mobilization convolved with connection probability. Average in the above area. So hazard area is basically the number of pixel where debris flow can occur and reach the interest cell (say Nhaz)... in the contributing area, times pixel area, and divided by the contour length, i.e. the square root of contributing area. Although I am confused because in Fig 2 : Hazard Area seem to be Nhaz times Pixel resolution (or Nhaz.a/sqrt(a)). But then smallest vales should be 0 and 30 (as it does in Fig 2). But in Fig 6 it goes from 0.1 to 1e3… So there seems to be a problem between the 2 definitions. Please check.
Your interpretation of SHALRUN-EQ is correct. The reason for sub-pixel hazard areas is due to multiple flow path routing. We now explain this more clearly (see L432).

L462: repeat from L452-453. Cut or rephrase ? **Rephrased to avoid repetition.**

L478-482 : Steepest descent may be too conservative, even if your rule needs to be simple, maybe you could mention that probability to propagate on non-steepest descent path is probably non-null.
This is an error in our explanation. We in fact use multiple flowpath routing, and amended our description of this in the methods section (see L435).
Also what about landslide large enough to be continuing beyond the first cell with angle below the deposition threshold? I see this is partially acknowledged in the discussion. Maybe you can flag here the fact you discuss such limits later. **We Agree and now point the reader to our discussion of this in section 7.1. (see L450).**

L512-516 : Ok, simplicity is important and it is difficult to integrate other effect mentioned here. But what about checking the actual evolution of probability with slope, for both initiation and stop? A reasonable estimate of scar area can be obtained by selecting the highest elevation pixel in your landslide, and selecting as many as needed to reach a scar area with an aspect-ratio of 1.5 (Domej et al., 2017) and a mean width representing of your polygon (see Marc et al., 2018 for how to do that). Doing so you could check if a plateau develop in your probability ratio after 39Æ or so... Interestingly you could reverse the idea and take the lowest N pixel (N ~ Width / 30 for 30m resolution DEM) of your landslides to obtain a probability of stopping.
We had performed this analysis with interesting results. We found that landslides initiate on a fairly narrow range of slopes but stop on a much broader range (consistent with our observations), with modal values similar to our optimized values. However, these results are telling us the slopes on which landslides initiate and stop rather than the probability of initiation and stopping given slope, so we need to be careful in connecting the two sets of results. A careful examination of this connection is outside the scope of the paper since we focus on developing simple rules.

L536 : Did you check the curve appearance when using gradients, that is tan(Theta) (with theta the slope in degree) ? Because the tan(theta) does appear mostly exponential over a large range of Theta. Thus a linear function of tan(theta) (the relevant parameter for landslide stability) may appear exponential when plotted against theta.
The kink in some curves at low slopes indeed suggested that tan(theta) might be a better predictor. While this is consistent with landslide mechanics, we found that for most inventories this relationship does not provide a good fit to the data at high slopes. Given the additional complexity of the tangent function it is not well suited to a simple rule so we chose not to report it here. However, the misfit between tan(theta) and landslide probability is clearly interesting and merits further examination in the future.

L538-542: Northridge and Haiti are shifted compared to other. They both become > average probability around 20Æ , vs 30 for others. This roughly correspond to modal slopes of these areas. It would be interesting to re-plot all curves not against slope, but slope – Sm the modal slopes. This collapsed curves on a similar analysis for rainfall (cf Marc et al 2018) Similarly is there a large variety of drainage area distribution ? Haiti and Northridge are very peculiar again compared to the other cases. Some normalization by the mode of the landscape drainage area may be important.
This is a good suggestion in terms of improving the explanation of the dataset as a whole but does not alter the simple rules because: 1) they are applied in relative terms (i.e. choose the location with the lower local slope); and 2) the alteration would require knowledge of the slope distribution for a location (which will not be available to most users). Nevertheless, we have now performed normalization on both slope and UCA. We include the figures in the supplementary information and briefly report the findings in the main text (L529).

L542-543: If you consider that Haiti and Northridge are more sensitive because they reach higher ratio it may be a confusion because of the lack of normalization (previous comment). It is plausible the relation between slope – Sm and hazard is similar, only the difference between resolvable slope (with a 30m DEM) and the modal slope is larger, allowing to reach larger relative hazard. I think the effect of normalizing for the landscape must be assessed.
This is exactly what the normalization shows. We have adjusted the text to reflect this observation, added a normalized panel to the figures, and refer to the normalized results in the text (L505).

L545: combined or merged PDF rather than amalgamated (that sounds negative an unusual to me but I may be wrong). **Altered to combined (L506).**

L555: You say you observe contributing area, but you have normalized by contour length. In the paragraph about hazard (L489), you say contour length is a^0.5, but it is not so clear what is a (the area of a cell, which cell ?) On Fig 2, contributing area seems to be the square root of a. It would be consistent with the contour length estimated as sqrt(a) but then why not say straight you look at the sqrt of drainage area ? Maybe I missed something, or it is worth clarifying a bit.
We now clarify this on first introducing upslope contributing area "and normalising by the grid cell width to minimise grid resolution biases" (L371), and in our definition of l_j, as the cell width (L461).

L562: This was somehow my expectation, so why not normalizing the contributing area and thus analyzing a/a_rc , with a_rc the channel ridge transition area? Like this the relative decrease or increase away from this objective characterization of the landscape could be analyzed (and the plot in Fig 3,4 would compare hazard curve shape only, not locations). This seems like an important improvement even if I understand that you may point to the fact a layman user of an hazard rule may not guess the modal slope of its landscape or the value of a_rc. After some analysis in the normalized domain general rules for the natural domain may be derived.
We agree, and now include a normalized plot showing the Northridge curve partially collapsing onto the other curves. Given the generally poor performance of upslope contributing area we choose not to come up with a new rule based around it, nor adjust the other rules in light of these results.

Fig 4 is very interesting and make a lot of sense after Fig 3. However, I am wondering about two things…
1/ Would all the plot look the same if you use normalized area and slope ? Maybe not given that it was not expected from Fig 3 that Finisterre would be different, but it seems worth and easy to check.
The differences that result from normalization are largely in the steepness of the surface rather than the way that slope and upslope contributing area interact. As a result there is little obvious change

in Fig 4 as a result of normalization. However, we show the normalized results in the supplementary information for completeness.

2/ You work with 100 log-bins of a and it seems 1degree bins of slope. So I wonder what is your typical number of DEM cells in each of your bins, and thus how statistically significant bins are… This is a detail as pattern are very consistent and a larger bin size would rapidly increase the amount of data.
We have applied the approach of Rault et al., extended to 2D, to indicate bins where the hazard is significantly different from the study area average. We flag that in the figure caption.

Fig 5 : Skyline angle is strongly uni-modal. So I would study all areas with a relative skyline hazard: Sky-Modal(Sky). The modal will account for difference in incision/relief between landscape. A potential outcome of such normalization may be that your case have all similar behavior for high skyline angle (increase and then plateau) but that Gorkha, Haiti, Northridge have a steep decrease below a certain angle while not the three others.
We tested the effects of normalization and as you suggest it does collapse the data to some extent. We find that normalization is particularly effective at aligning the Gorkha, Haiti and Northridge hazard curves with those from the other sites. We now describe this normalisation in the text.

The definition you take for hazard area gives 0 hazard area for the reference in all cases and then a decrease. It does not seem that shift in the horizontal direction would do any good, and the vertical shift seems due to the proportion of zero hazard area in the landscape, so maybe computing a landscape PDF ignoring the zero would be insightful?
We suspect that normalisation may not be particularly informative in this case. We could normalise the initiation and stopping angles but we are then farther from a simple rule and, particularly in the case of stopping angle, it is not entirely clear what the appropriate property to normalize by would be. As a result we do not pursue normalization for hazard area.

L645: Ah<1 mÇ/m . I am surprised by this threshold, but maybe it is a typo. I would have say in Fig 5b the curves steepens most in all case around 20. It is true that for Haiti, Gorkha and Northridge there is a slight increase in the trend after Ah~1, but minor compare to the later steepening.
This was a typo, and has now been fixed.

Also to be sure that the difference between a peak or a plateau is a real result it would be important to check the evolution of the uncertainty in your last bins, where certainly few data are available (even if we cannot read the probability of Ah>1e2 or 1e3).
A peak followed by a decline in hazard with increasing hazard area is retained within that part of the data where there are sufficient observations to allow confident hazard identification only for Haiti. However, we have adjusted our plots to indicate which observations are more or less certain, using the approach of Rault et al. as described above, and discuss this in the modified text at L630.

We also do not see the difference in availability of such high hazard area in the different areas, so could a very low availability of such hazard areas in Haiti and Northridge (that have less steep slopes) caused a scattered behavior for Ah>100 instead of Ah>1000. A quantification of uncertainty may clarify that. See major comment. **Your suggestion that the earlier onset of scatter in Northridge and Haiti hazard curves is likely to reflect a lower availability of such steep slopes is supported by the Rault et al. analysis, which clearly identifies the point beyond which the curves become more scattered as the point beyond which hazard cannot be confidently resolved. We make this point in the main text at line 636.**

L672 : This sentence confused me. Do you mean each of the three parameters, may be better than the skyline angle for at least one event ? **Yes, your interpretation is correct. We think the confusion was due to a punctuation error (full stop should have been comma), and we have now fixed this.**

L674: These values do not match Table 1 with 0.72, 0.69, 0.74.... Please correct one or the other. **Thanks for spotting this typo, we have now fixed it.**

L694: I am a bit surprise by the term of channel inside this rule. I guess it derives from the fact that the hazard consider upslope contributing areas defined from flow algorithm. But the hazard area at many intermediate locations on hillslopes may be a channel for your analysis but not for the resident and deciders of the area. Because a channel is defined on finer scale than the DEM. You already say that this metrics is anyway difficult to estimate and handle for application, but this terminology would also complexify the problem for deciders or policy makers.

We can understand your concern here and have considered alternatives. However, we have chosen to retain the word channel within the rule for two reasons. First, because we feel that it is important to capture the notion of convergence and we are unable to find an alternative wording that can do so. Second, because we expect that if SHALRUN-EQ is calculating convergence using a 30 m DEM, it is extremely unlikely that the real topography does not have some sort of channel or gully within that area. It's hard to imagine a topography that would be convergent at 30 m scale but not obviously channelised or gullied at finer scales.

L699 : This is fortunate indeed, almost surprising.
Agreed - we expected more sensitivity to the parameters here.

L711: Interesting. Do you think this could be somewhat validated by making skyline and hazard graph for landslide above and below a certain threshold (say 5e3 m2 or even better above a certain width...) ?
This is an interesting idea and something that we will investigate in future but we feel that it is outside the scope of the current paper.

L739 : You certainly mean Meunier 2008 here. However, note that the new study from Rault et al., 2018 is considerably nuancing these past studies.
Modified to add citation and account for Rault et al's work (L727).

L820: And even for a trained observer.
Agreed but given our simple rules focus we choose to retain the focus on untrained observers here.

L822-23: I do not understand what you mean by "we expect the length scales over which this occurs to be long (order kilometres) relative to the other factors examined here" Do you mean that main lithological units are usually big (regional scales) and thus significant part of a landscape will have homogeneous lithology, whereas topographic attribute change at the scales of 10s of meter ? Then it is the length scale for the variability of lithology that you want to mention. Anyway please clarify.
Your interpretation is correct but we have clarified our point in line with your suggestion (see L812 in revised manuscript).

On a side comment, normalizing each landscape slope by their modal slope would be somehow a step toward normalizing difference in landscape that can be due to major lithological or geomechanical attributes (Korup 2008).
Agreed, but as discussed above including this in a simple rule would be problematic.

L824-826: This is an important and natural point to make but I would mention rainfall induced landslides straight here, as area affected by coseismic landslides are often even more often affected by rainfall induced landslides (at least for wet climate Nepal,Finisterre, Taiwan).
Agreed, and we have modified this text to: 'such as flooding or even rainfall induced landsliding'. (L815).

L830: And they likely do, given that large landslide (likely to travel further away as you recall in the introduction) are usually reported closer of the fault or at larger shaking values (Khazai and Sitar (2004), for the Chi-Chi earthquake (1999), Massey et al. (2018) for Kaikoura or Valagussa et al 2019 for systematic evaluation of PGA and landslide size distribution. So future exploration of the behavior of your hazard curve split for specific lithology of different area class should be done.
Agreed, both landslide size and lithology are interesting topics for future work but are outside the scope of this paper.

L834 : I would say we can reasonably expect strong differences : given that hazard increase strongly with local slope for EQ (Fig 4) but not for the rainfall induced landslides : as shown by the anaysis similar to your Fig 3 in Marc et al., 2018. Further, the longer runout (due to lower stopping angles) and stronger dependence on contributing areas are additional changes.
We agree that large differences are possible, but we think it is fair to say that the strength of these differences is not yet clear.

References used in the review

Claire Rault, Alexandra Robert, Odin Marc, Niels Hovius, and Patrick Meunier, Seismic and geologic controls on spatial clustering of landslides in three large earthquakes, 2018, https://www.earth-surf-dynam-discuss.net/esurf-2018-82/
Marc, O., Stumpf, A., Malet, J. P., Gosset, M., Uchida, T. and Chiang, S. H.: Towards a global database of rainfall-induced landslide inventories: first insights from past and new events, Earth Surface Dynamics Discussions, (March), 1–28, doi:10.5194/esurf-2018-20, 2018.
Maufroy, E., Cruz-Atienza, V. M., Cotton, F. and Gaffet, S.: Frequency-Scaled Curvature as a Proxy for Topographic SiteEffect Amplification and Ground-Motion Variability, Bulletin of the seismological society of America, 105(1), 354–367, 2015
Valagussa, A., Marc, O., Frattini, P., and Crosta, G. B.: Seismic and geologic controls on earthquakeinduced landslide size, Earth and Planetary Science Letters, 2019. https://doi.org/10.1016/j.epsl.2018.11.005
Bijan Khazai, Nicholas Sitar, Evaluation of factors controlling earthquake-induced landslides caused by Chi-Chi earthquake and comparison with the Northridge and Loma Prieta events, Engineering Geology, 2004, https://doi.org/10.1016/S0013-7952(03)00127-3 .
Domej, G., Bourdeau, C., and Lenti, L.: Mean Landslide Geometries Inferred from a Global Database of Earthquakeand Non-Earthquake-Triggered Landslides, Italian Journal of Engineering Geology and Environment, 87–107, https://doi.org/10.4408/IJEGE.2017-02.O-05, 2017
Korup, O. (2008), Rock type leaves topographic signature in landslide -dominated mountain dominated mountain ranges, Geophys. Res. Lett., 35, L11402, doi: 10.1029/2008GL034157.

Reviewer 2

General Comment

Thank you for this interesting paper. Using six inventories of coseismic landslides, the authors test the significance of multiple topographical parameters to constrain a set of simple rules in order to minimise exposure to landslide hazard. The paper forms a significant added value to the landslide hazard scientific community as a first attempt in identifying simple rules which is essential for communication about complex hazards to a broad (lay) audience in creating awareness and minimizing landslide exposure. I appreciate the authors' balanced conclusion on the most effective parameters for hazard reduction ["We conclude that decisions on how to reduce landslide hazard most effectively need to be made on a case by case basis, and are best made using hazard area, skyline angle, and the local slope in conjunction with each other."], unfortunately this is not taken in the abstract and conclusion where the authors present without further nuances three simple rules. The discussion is focused on the authors' results with limited reflections with respect to related research (cf. introduction). I believe such a reflection would make the results more convincing.

Thank you for your careful reading of the paper and your many helpful comments and suggestions. We have worked hard to identify this set of simple rules and it is encouraging that this comes through in the manuscript. However, we will take on board your suggestion to temper our presentation of these rules. We have sought to clarify that we are suggesting such rules as a new tool to complement existing approaches rather than replace them. We highlight, though, that we are clear from the outset that the rules are designed to complement other approaches. For example, we say in the abstract: "Our simple rules complement, but do not replace, detailed site-specific investigation; they can be used for initial estimation of landslide hazard or guide decision-making in the absence of any other information."

Specific Comments

The first time I read through the paper I found the abstract and introduction confusing while the terms hazard, exposure, risk, hazard response, "anticipating". . . are used without first clearly constraining them. Even though the audience from NHESS should be familiar with these terms I believe that these terms are still easily confused. I would therefore recommend to distinguish these terms in the introduction, or make reference to literature in which this is done.

Thank you for this useful feedback. We had been careful to define key terms such as hazard, exposure, risk and mitigation in the introduction and were even concerned that these definitions hampered the flow of the text, so it is helpful to know that they are important. We generally define terms in the introduction rather than the abstract given the limited space in the abstract. In all these cases we give the definition within five lines of introducing the term, though to retain the flow of the text our definitions are generally 'in-line' rather than taking the form of a separate sentence in the form 'x is defined as…'.

However, following your comment we have sought to simplify our language, removing hazard response (and instead talking in terms of risk mitigation, which we introduce earlier).

The paper is well structured and the figures of high quality presenting very clearly the results, yet I would suggest to shorten the paper to bring forward the main messages even more clearly. Sections that I would suggest to reduce are section 4 ("Earthquake inventories") by providing a summary of the used inventories with the most important parameters necessary for the analysis; and section 5 ("Methods") could also be reduced, moreover this would allow the reader to more easily follow the workflow.

We are pleased that you found our presentation of the results clear. We have considerably shortened the "Earthquake inventories" section of the manuscript and slightly shortened the Methods section.

I wonder how easily the presented rules can be adopted without prior knowledge or skills, which seems to be the main purpose of the study yet lacking from the discussion. This is not easily answered and out of scope of the study to check the applicability of their rules by householders, local government, and NGOs, but I would recommend to be more cautious when claiming to present 'simple rules'.

We have chosen the term 'simple rules' to make the connection to an existing and active field of research around heuristic decision-making (e.g. Gigerenzer, 2008). This field explicitly refers to heuristics as 'simple rules' (e.g. Todd and Gigerenzer, 2000, Behavioral and brain sciences, 23(5):727-741). We would argue that the first two rules are simple and do not require prior

knowledge or skills: ‘minimize your maximum angle to the skyline’ and ‘avoid steep (>10˚) channels with many steep (>40˚) areas that are upslope’.
Your point here and in detailed comments that the language of the third rule needs to be improved is helpful and we have simplified this rule to read: ‘minimise the angle of the slope under your feet, especially on steep hillsides, but not at the expense of increasing skyline angle or hazard area’.

Examining the applicability of these rules is, as you suggest, beyond the scope of this study, but that doesn’t prevent the development and testing of the rules themselves from being a useful exercise. We have had some experience of applying these rules with organisations involved in post-earthquake reconstruction in Nepal, and have some positive feedback so far, but it is too early for a more formal evaluation and we feel strongly that this would be the topic of another manuscript.

<u>Detailed comments on “Simple rules to minimize exposure to coseismic landslide hazard”</u>

L10 - The abstract misses information on the fact that the study is on coseismic landslide hazard.
Agreed, added ‘coseismic’ on line 15.

L15 - Do you present in the end primarily simple rules to identify hazard? Or rules to minimize exposure, cf title? I understand they go hand in hand, but it would be good in my opinion to be aware that the terms Hazard, Exposure and Risk are easily confused by readers. Being consequent in using terminology in the abstract might avoid confusion.
Thank you for spotting this possible source of confusion. Although the metrics identify hazard, we have written the rules in such a way that they provide advice on action to take to minimize exposure. We have modified this sentence on line 15 the abstract to be consistent with the title.

L18 - Not sure what you mean with "as a proxy for hillslope location".
We added: “…location relative to rivers or ridge crests.” (L18).

L20 - From reading only the abstract it is difficult to agree that defining "the upslope area with slope >39° that reaches a location without passing over a slope of <10°" does not require prior knowledge or skills and that it is easy understandable.
Agreed, but on line 26 we distil this into a simpler rule: ‘avoid steep (>10˚) channels with many steep (>40˚) areas that are upslope’

L22 - Could you add the observation period covered by the inventories here between brackets to know what is 'recent' to you?
Added: “… earthquakes (occurring between 1993 and 2015)” (L23)

L23 - Show which other metrics were tested besides the two new metrics you introduce so this sentence ("most skilful") has more meaning.
We mention these on lines 16-17 and are conscious that we are short on space in the abstract. The text now reads: “We examine rules based on two common metrics of landslide hazard, local slope and upslope contributing area as a proxy for hillslope location relative to rivers or ridge crests. In addition, we introduce and test two new metrics…” (L17)

L25 - If the rules should be simple and applied by people without skills, why not round to 40°? What is the sensitivity of this rule to a change in the slope of one degree?
Agreed, we will round to 40 degrees, the impact on performance of a one degree change is negligible.

L26 - How does that work, "minimise local slope especially on steep slopes"?
It is particularly important to minimize local slope on steep slopes. This is explained in more detail in the results and discussion sections. We are not sure if you found the sentence difficult to interpret or were concerned about how robust the finding was. The latter will be addressed in the results and discussion section of the paper. We have added a comma between the clauses and altered the second ‘slopes’ to ‘hillsides’ to help to clarify the meaning of the phrase (e.g. L28).

L26-28 - This rule seems dubious when stating at the same time "even at the expense of increasing upslope contributing area" and " but not at the expense of [...] hazard area" with the latter also comprising upslope contributing area.
The hazard area is found within the upslope area but these two metrics are radically different from one another, as we show in the paper. Our results strongly support both parts of this rule that you identify above.

L38 - I would suggest to use the updated paper of Petley, 2012:
Froude, Melanie J., and D. Petley. "Global fatal landslide occurrence from 2004 to 2016." Natural Hazards and Earth System Sciences 18 (2018): 2161-2181. Given the very extensive reference list I think that 'e.g. Froude et al. 2018' would do while omitting the other references if not necessary in the rest of the paper.
Agreed. Added.

L46 - I think "respond to that hazard" is of lesser relevance here as you do not deal with hazard response in this paper.
We agree that response is not our focus, but information at a scale that enables decisions to be made on how to respond to the hazard is one of the key motivations for this work. Thus we think it is important to retain the response clause.

L55 - I would add to “site-specific information that may not be available” something like "such as... " to make it more informative.
Agreed, changed to “…available (such as geological maps or landslide inventories)”. (L56)

L62 – “hazard maps cannot resolve hazard at those scales” : I doubt that, with the current availability of high-resolution remote sensing data; yet I agree it could be time-consuming.
Agreed, although it is worth highlighting that we are talking about national and regional scale maps in this clause. We softened the statement by changing from “cannot” to “do not”. (L64).

L97 - How does the “self-recovery” relate to the first part of the sentence? I don't see the relevance of it here.
We added an inline indication of what self-recovery means “…self-recovery after disasters (for example, via reconstruction programmes in which householders rebuild their own homes)”. (L100).

L102 - Not only of “less use” but also inherently different; your rules aim to minimize landslide exposure, not to help in hazard response. Please modify.
We disagree with this point. Action to minimize your exposure to a hazard can occur both before and during an earthquake. Taking the earthquake example, this might be the difference between relocating away from an earthquake prone area and choosing to ‘drop cover and hold on’. Given this, we think that ‘less use’ is the appropriate modifier here.

L107 - Could you site a reference at the end of this sentence, in order to make "our" refer to the scientific background.
Here, the use of ‘our’ was referring to the findings of this paper. To clarify this, we modified “Some of our results may be transferrable to landslides caused by more frequent triggers, such as storms, and we consider this point in the discussion.” To “We consider the extent to which our results may be transferrable to landslides caused by more frequent triggers, such as storms, in the discussion.” (L109).

L110 - Add respective countries between brackets.
Modified to: “Finisterre (Papua New Guinnea), Northridge (USA), Chichi (Taiwan), Wenchuan (China), Haiti, and Gorkha (Nepal) earthquakes”. (L114).

L112-116 - I don't see much difference between the two questions?
The first relates to absolute performance of the rule set, the second to relative performance of rules within the set. We have added this sentence on L121 to clarify this point.

L116 - What kind of patterns? Temporal/spatial... **modified to “spatial patterns”. (L122).**

L118 - Which "combined datasets" you refer to? The landslide inventories or more specifically to the derived topographical parameters from the inventories? **Modified to “landslide datasets”. (L124).**

L127 – This question is probably related to my lack of knowledge in the earthquake-triggered landslides, but to me it is not clear what you mean here with 'local slope', could you specify? Do you mean the slope at the landslide head ? What is the spatial extent of a "local" slope?
We have now clarified our definition of local slope, which although conventional may not be familiar to all readers: "Local slope, the gradient of the ground surface measured over some short distance (usually ~1-100 m)" (L133).

L129 - In Parker et al. 2017, who you cite, they find hillslope gradient as an important driver, which is different than local slope I would think? Parker et al. 2017: "We find that a simple model combining PGA and hillslope gradient provides the most numerically elegant and best fitting model. The use of topographic variables other than hillslope gradient were found to produce models with a lower fit,..."
In fact we use 'local slope' to refer to the same property that Parker et al. 2017 call hillslope gradient. We considered a switch to their nomenclature but feel that local slope is the best established and most appropriate term for the property that we refer to. One reason for this is that local slope indicates that a gradient is being calculated over a (relatively) short length scale rather than over the entire hillslope (from ridge to river). It is also more clearly contrasted with a non-local measure like skyline angle, which considers the topography over a larger window around a particular point of interest. We now clarify this by defining local slope within the sentence (on L133) as mentioned above.

L135 - Can you add a reference here, after "However, shaking for any future earthquake cannot be predicted due to lack of certainty on source location, magnitude, rupture style, and local site effects. **Added on L142.**

L194 - How is this "non-local" when accounting for local slope?
The hazard area is a non-local metric because the value of the metric at a given cell is a function of cells within a wider neighborhood than only its 8 connected (local) neighbors. In this case the property is the gradient (local slope in our terms) of the cells in this wider neighborhood (from all possible initiation points to the target cell).

L323 - "conditional probability for landslide occurrence" seems more informative to me.
Agreed, but we are talking about a broader class than simply occurrence. We have modified the title to: "Conditional probability and landslide hazard" (L268)

L324 – "Landslide hazard can be defined as…" should already have been clear from the introduction.
Agreed, but here we are building the case for a conditional probability based analysis, so we feel that the connection with the definition of landslide hazard needs to be retained here.

L342 - Make reference to preceding research using this approach, yet using rainfall characteristics (I,D) instead of landslide susceptibility (a). E.g., Berti, M., Martina, M. L. V., Franceschini, S., Pignone, S., Simoni, A., & Pizziolo, M. (2012). Probabilistic rainfall thresholds for landslide occurrence using a Bayesian approach. Journal of Geophysical Research: Earth Surface, 117(F4).
Agreed, this is a useful reference and while many other studies apply similar approaches this has a stronger connection than most. We have added: "…landslide inventories. This type of approach has proved successful for a range of applications including identifying topographic controls on vegetation patterns [Milledge et al., 2012] and the rainfall conditions that trigger landslides [Berti et al., 2012]. If we grid…" (L289).

L383 - I would strongly reduce this section as readers of NHESS could be assumed to be acquainted with the concept of ROC curves. **We feel that a clear explanation of ROC curves is important in this paper because of the central role that these curves play in quantifying the performance of the metrics that we test.**

L396 – "the naïve (random)" : Necessary to repeat (L394) the two terms here again?
Agreed, removed '(random)' on L356.

L402 - Why would you use NED elevation data? Since SRTM covers each of the inventory, it seems more logical to use consequently the same DEM source to avoid bias. Certainly because you emphasize on the

slope factor here, there should not be a biased introduced voluntarily (unless it would be used for an investigation of sensitivity to spatial resolution)
Our approach was to use the best freely-available data at each location, but to use a consistent resolution between sites. For all the locations but Northridge SRTM is the best quality available data. This can be problematic, as SRTM data can have gaps (as in Wenchuan) and can smooth highly dissected terrain (as in Northridge). While in Wenchuan we had to restrict our analysis to a subset of the terrain, in Northridge we were able to use better topographic data (the NED), though we downsampled to the same resolution. Our performance tests at Northridge, comparing SRTM and NED data, support this. We find a considerable performance reduction for SRTM relative to NED data, particularly for the hazard area metric. This is likely due to the highly dissected topography within the Northridge study area; the SRTM data do not capture this topography but the resampled NED data do.

L416 - Avoid repetition, cf. L181
Addressed by modifying and shortening sentence.

L420 - Could you clarify what you consider here as channel and channel spacing? How is channel spacing related to the skyline?
Channel spacing is related to the window size required to evaluate the skyline angle because the skyline is likely to be defined by local ridges and the distance to these ridges to be defined by channel spacing. However, the term was distracting and in retrospect unnecessary so we have removed it in our new explanation.

L421 - What is meant with 'characteristic hillslope length'?
Characteristic hillslope length can be interpreted as an estimate of the average hillslope length for the study area. It is calculated based on the upslope area at which there is a scaling break in the relationship between slope and upslope area following the approach of Roering et al. (2007). We have now replaced 'characteristic' with 'average' since this is a more straightforward term (L382).

L423 - What is the relation between the characteristic hillslope length and channel spacing?
Since channels are separated by ridges with hillslopes on each side, then the average channel spacing is twice the characteristic hillslope length. In answering this query we identified an alternative explanation for our choice of search radius that avoids the confusing connection to channels.

L422-423 - Since these are parameterized by the chosen inventories, do you estimate that your rules might change for other areas? Or do you argue that the conservative approach is general enough?
The size of this window should not have an impact on the rules. It will affect only on their implementation and testing within a GIS. The objective here is to ensure that the search radius is large enough to reproduce the same horizon angle in the GIS that would be measured in the field.

The four comments above suggest that our explanation of our choice of search radius for the skyline angle was a source of confusion. We have now rephrased the entire section as follows (removing reference to channel spacing which was a distraction):

"For each cell in a study area, we estimate the skyline angle by calculating vertical angles between the target cell and every other cell within a 4.5 km radius. This search radius is chosen to greatly exceed the average hillslope lengths in all study areas and thus to fully capture the local skyline. The longest average hillslope length out of our study areas is ~500 m for Wenchuan, estimated following the method of Roering et al. (2007). We choose a search radius nine times larger than this hillslope length to ensure redundancy in capturing the local skyline and because the only disadvantage of a larger radius is increased computational cost." L380-386.

L423 – The sentence "We choose larger window size because skyline angle estimates become asymptotically insensitive to window size" is not clear to me, larger than what?
This sentence has been removed from the modified manuscript.

L437 - Seems to be projected from point P?
Agreed, altered.

L443 - With “non-local” you mean not at the landslide initiation location?
This point has been addressed in our earlier discussion of ‘non-local’.

L464 - Avoid repetition with L453.
Modified to remove repetition.

L547-548 - "on which people generally choose to live" : This statement is too vague to me without a reference, does this statement reflect to your inventories solely?
We can be confident of this for our specific inventories but would argue that it is true in general. However, we do not have a reference to support it, so we have adjusted the sentence to refer to our inventories in particular (L509).

L567 - I do not see a significant difference in the point density (~number of observations) for observations with Upslope contributing area > 1000m./m.
Our point here was that the number of observations per bin was very small for upslope contributing area >100 m^2/m. However, we have adopted a new approach (as suggested by reviewer 1) that enables us to identify the point at which sample sizes per bin are too small to confidently interpret.

L631- Make reference to the respective equations in the Methodology section for the parameters mentioned here.
Agreed, equation references added (L615).

L673- None, capital N. **The typo was the full stop, which should have been a comma. This is now fixed.**

L677 - Table 1 and Fig. 6 are redundant, you could add Fig. 6 in supplementary material?
We disagree, and feel that Fig.6 shows the data that are synthesized in Table 1. It is important for readers to see these curves rather than the AUC values only, both because they illustrate the point more clearly than a table of values and because they provide richer information. As a result, we feel that it is important to include this in the text rather than leaving it for the supplementary info.

L753-756 – I think it is very valuable that the authors take a step back from there rules while summarizing the main parameters to take into account for hazard assessment, being “hazard area, skyline angle, and the local slope in conjunction with each other”. Yet this idea that is stated as a conclusion “We conclude that decisions on how to reduce landslide hazard most effectively need to be made on a case by case basis, …” is not repeated in the abstract or conclusion, which to me is confusing. It is even in contrast with the conclusion stating (L858-859) “suggesting that the average parameters can be applied to other inventories. These findings can be distilled into three simple rules:”.
The ‘case by case basis’ on L754 refers to application of the rules on a case by case rather than simply resolving to always move upslope or downslope for example. This does not conflict with our later conclusions. However, we have modified the sentence on L753 (now L742) to remove the word conclusion and thus avoid confusion.

L764-L766 I am not sure what your message is here, helping in decision-making before an earthquake is the same to me as decision making after an earthquake which is in turn also before a future earthquake. What is the differentiation that I am missing here?
The point we are trying to make here is that these rules could be used not only for long-term decision making, where the time that it takes to move a certain distance is not the limiting factor in whether you can locate yourself or your assets, but also for short-term decision making during or in the immediate aftermath of an earthquake when one may only be able to move short distances. We clarify this in our revised manuscript (L752-755).

L770 - This statement is largely depending on which spatial extent you perform your analysis and therefore I don't think it is relevant, or should be said in a different way.
Agreed. The sentence order has now been adjusted so that this statement (L759) follows the sentence on the granularity of landslide hazard and is supported by examples in two subsequent sentences.

L849 - In "the highest area at a given slope" it is not clear what you mean with "highest area".

Agreed, and this has been rephrased to “largest upslope contributing area” (L735).

Simple rules to minimize exposure to coseismic landslide hazard

David G. Milledge[1], Alexander L. Densmore[2], Dino Bellugi[3], Nick J. Rosser[2], Jack Watt[2], Gen Li[4], Katie J. Oven[2]

1. School of Engineering, Newcastle University, Newcastle upon Tyne, UK

2. Institute of Hazard, Risk, and Resilience and Department of Geography, Durham University, Durham, UK

3. Department of Geography, University of California, Berkeley, USA

4. Division of Geological and Planetary Sciences, California Institute of Technology, Pasadena, USA

Abstract

Landslides constitute a hazard to life and infrastructure, and their risk is mitigated primarily by reducing exposure. This requires information on landslide hazard at a scale that can enable informed decisions. Such information is often unavailable to, or not easily interpreted by, those who might need it most (e.g., householders, local governments, and NGOs). To address this shortcoming, we develop simple rules to minimize exposure to coseismic landslide hazard that are understandable, communicable, and memorable, and that require no prior knowledge, skills, or equipment to apply. We examine rules based on two common metrics of landslide hazard, local slope and upslope contributing area as a proxy for hillslope location relative to rivers or ridge crests. In addition, we introduce and test two new metrics: the maximum angle to the skyline and the hazard area, defined as the upslope area with slope >40˚ from which landslide debris can reach a location without passing over a slope of <10˚. We then test the skill with which each metric can identify landslide hazard – defined as the probability of being hit by a landslide - using inventories of landslides triggered by six earthquakes that occurred between 1993 and 2015. We find that the maximum skyline angle and hazard area provide the most skilful predictions, and these results form the basis for two simple rules: 'minimize your maximum angle to the skyline' and 'avoid steep (>10˚) channels with many steep (>40˚) areas that are upslope'. Because local slope alone is also a skilful predictor of landslide hazard, we can formulate a third rule as minimise the angle of the slope under your feet, especially on steep hillsides, but not at the expense of increasing skyline angle or hazard area'. In contrast, upslope contributing area, has a weaker and more complex relationship to hazard than the other

Deleted: Department
Deleted: Earth
Deleted: University of Southern
Deleted: , Los Angeles
Deleted: ¶
Deleted: about how to respond to that hazard.
Deleted: government
Deleted: identify
Deleted: evaluate
Deleted: , and
Deleted: 39˚ that reaches
Deleted: -
Deleted: recent
Deleted: 39˚
Deleted: '
Deleted: local
Deleted: slopes and even at the expense of increasing upslope contributing area
Deleted: Upslope contributing area, by

predictors. Our simple rules complement, but do not replace, detailed site-specific investigation; they can be used for initial estimation of landslide hazard or to guide decision-making in the absence of any other information.

Keywords: coseismic landslides, landslide, heuristic, hazard, exposure

1. Introduction

Landslides involve the downward movement of soil or rock under gravity, sometimes mixing with water or air to run out rapidly over long distances. Landslides have considerable destructive potential and constitute a major hazard to life and infrastructure (e.g. Froude and Petley, 2018).

Deleted: Alexander 2005; Petley, 2012; Klose et al., 2016; Mertens et al., 2016

Landslide risk can be mitigated by either reducing exposure - the likelihood that a particular person or structure is hit by a landslide - or by reducing the consequences of landslide impact. The latter is expensive for a building (Fell et al. 2005; Volkwein et al., 2011; Guillard-Gonçalves et al., 2016) and extremely difficult for a person (Kennedy et al., 2015). As a result, efforts in reducing landslide risk tend to focus on reducing exposure, primarily by siting infrastructure and assets (or by choosing to spend time) in places of lower landslide hazard. These choices, however, require information on landslide hazard at a scale that can enable informed decisions about how to mitigate the risk. In other words, a decision to reduce landslide exposure requires knowledge of how landslide hazard varies in space.

Deleted: Petley, 2012,

Deleted: respond to that hazard.

Quantitative landslide hazard information is commonly expressed as a relative weighting or probability of landslide occurrence in a given location and over a specified period of time. This is often communicated as a hazard map (Dransch et al., 2010). These maps can provide useful information to inform decisions such as siting infrastructure, allocating resources, designing countermeasures, or planning mitigation measures such as evacuation routes. There are, however, at least five limitations to reliance on hazard maps as the sole source of landslide hazard information. First, landslide hazard maps do not exist for all hazardous locations, since their generation requires technical expertise and site-specific information that may not be available (such as geological maps or landslide inventories). Second, where maps do exist they may not be available to those that need them. Whether in physical or digital form, hazard maps are rarely held by the communities that live

Deleted: .

within their boundaries (Alexander, 2005; Mills and Curtis, 2008; Twigg et al., 2017). Third, where landslide hazard maps are available their resolution may not be fine enough to address the questions that potential users will have. In everyday decisions, from where to build a house to which way to walk, distances of even a few metres can matter greatly for determining landslide exposure, because landslide hazard can vary substantially even over those short length scales. National- or even regional-scale hazard maps do not resolve hazard at those scales, however, and hazard maps at the appropriate scale would be extremely costly and time-consuming to produce over large areas. Fourth, landslide hazard maps are designed for technical users (such as engineers and planners) and thus can be difficult for non-technical users to interpret (Dransch et al., 2010). Hazard is often expressed in probabilistic terms which are inherently difficult to communicate and understand (Thompson et al., 2015). The maps may also require particular equipment, such as a computer with appropriate software, or additional contextual information to enable clear visualisation or to orient the user (Mills and Curtis, 2008). Finally, landslide hazard maps may lack appropriate information for decision-making. For example, landslide hazard is commonly equated simply with the probability of landslide initiation at a given location, rather than the probability that that location will be impacted by a landslide occurring there or somewhere upslope.

In the absence of detailed hazard maps, how should we make decisions about siting infrastructure or spending time in landslide-prone areas? An alternative, and complementary, form of hazard information might be a set of general rules that can be memorised by anyone who might be exposed to landslide hazard, or by those charged with managing landslide risk, to be applied where no other information exists. A good general rule should: 1) be understandable, communicable and memorable; 2) require no prior knowledge, skills or equipment to evaluate; 3) be a skilful discriminant of hazard; and 4) be cast so that it does not increase exposure to another hazard. A good example of such a rule would be the instruction to minimise exposure to tsunami: “in case of earthquake, go to high ground or inland” (Atwater et al., 1999, p20). Research has shown that these types of simple rules are already to some extent implicitly coded into the decisions that people make (e.g., Gigerenzer, 2008), reflecting tacit knowledge of hazards (e.g., Shaw et al., 2008; Lebel, 2013; Twigg et al., 2017). Importantly, however, there are limits to this tacit knowledge (Briggs, 2005); in particular, the body of experience required to generate these rules is limited by both the infrequency

Deleted: . Landslide

Deleted: varies

Deleted: very

Deleted: (tens of metres), but national

Deleted: cannot

Deleted: ,

Deleted: is

Deleted: .

Deleted: .

of triggering events, such as earthquakes or large storms, and a focus on *normal* rather than *unusual* but not improbable events, which can introduce bias (McCammon, 2004; Kahneman and Klein, 2009). For example, while perennial rainfall-triggered landslides and the risks that they pose may be familiar to people in landslide-prone communities, landslides triggered by large earthquakes may fall outside of residents' lived experience, and so will be more challenging to comprehend and account for in decision-making. If simple, memorable rules (fulfilling criteria one and two above) could be derived from a large inventory of hazardous events, these biases might be reduced while maintaining the other benefits of a rule-based approach (criteria three and four). Such a set of data-based rules could be used in the absence of, or in conjunction with, existing tools such as hazard maps and local knowledge, both to inform decisions and to inspire discussion amongst householders, local government, and non-governmental organisations. Such knowledge is commonly in demand not only from technical users but also from lay people (Twigg et al., 2017; Datta et al., 2018), especially because self-recovery after disasters (for example, via reconstruction programmes in which householders rebuild their own homes) is increasingly recognised as a critical mechanism of recovery (Twigg et al., 2017).

Here we focus on rules that can be derived from the topography surrounding a given location and that differentiate exposure to coseismic landslide hazard on length scales of tens to hundreds of metres. Such rules are likely to be most useful for decisions before an earthquake about where to site infrastructure or spend time, and may be less useful for decisions about where to go during an earthquake when time is limited. We focus on earthquakes because landsliding is an important, but poorly understood, aspect of hazard in many recent continental earthquakes (Huang and Fan, 2013; Roback et al., 2018). We consider the extent to which our results may be transferrable to landslides caused by more frequent triggers, such as storms, in the discussion.

We examine candidate rules based on our existing understanding of landslide mechanics to identify those that meet criteria one and two above. We then test the skill with which each candidate rule can identify landslide hazard, using inventories of coseismic landslides from the recent Finisterre (Papua New Guinea), Northridge (USA), Chi-Chi (Taiwan), Wenchuan (China), Haiti, and Gorkha (Nepal) earthquakes. Our goal is to determine the rule or rules that best fulfil the four criteria listed above, and that therefore provide the best combination of simplicity and skill in anticipating coseismic

Deleted: introducing biases
Deleted: a scale
Deleted: of
Deleted: use
Deleted: 2017). Some of
Formatted: English (United States)
Deleted: and we consider this point
Formatted: English (United States)
Formatted: English (United States)
Deleted: ,
Formatted: English (United States)
Deleted: , Chichi,
Formatted: English (United States)
Deleted: ,
Formatted: English (United States)
Formatted: English (United States)

landslide impacts. We ask two key questions: (1) to what extent could observed landslide locations in past earthquakes have been predicted by these simple rules alone, without recourse to more complex models; and (2) is there a single rule or set of rules that performs well across all earthquakes, and could form the basis for anticipating landslide-affected locations in a future earthquake? The first question relates to the absolute performance of the rule set, while the second relates to relative performance of rules within the set. While spatial patterns of landsliding in these earthquakes have been previously established, this is to our knowledge the first attempt to extract a more general set of rules from landslide datasets across multiple earthquakes.

This paper is necessarily technical, addressing the question of whether it is possible to formulate such rules, identifying which rules work best and assessing their performance. We therefore expect the paper's primary audience to be technical experts with an interest in landslide risk reduction. We have begun to explore ways of expressing these rules in a format that is more accessible to a general audience (e.g. Milledge et al., 2018).

2. Potential predictors for coseismic landslide hazard: slope and upslope contributing area

Local slope, the gradient of the ground surface measured over some short distance (usually ~1-100 m) has been identified as an important driver of landslide occurrence in almost all prior landslide studies (e.g. Harp et al., 1981; Tibaldi et al., 1995; Keefer, 2000; Wang et al., 2003; Xu et al., 2012, 2013; Parker et al., 2017). This is consistent with mechanistic expectations based on the balance of driving and resisting forces on an inclined failure plane (Taylor, 1937). Local slope is an intuitive parameter that is familiar to most people and can be easily estimated in relative terms (i.e., hillside A is steeper than hillside B) without specialised equipment. Seismic acceleration or shaking is commonly identified as the other dominant control on coseismic landslide occurrence (Khazai and Sitar 2004, Meunier 2007). However, shaking for any future earthquake cannot be predicted due to lack of certainty on source location, magnitude, rupture style, and local site effects (Geller, 1997). It is therefore difficult to incorporate into a general rule for future landslide hazard.

Ridges are often considered to be areas of high coseismic landslide probability due to topographic amplification (Densmore and Hovius, 2000; Meunier et al., 2008; Rault et al., 2018), while rivers are

Deleted: While

Deleted: the combined

Deleted: Shaking intensity

Deleted: .

Deleted: .

by definition areas of flow concentration into which landslides from multiple potential initiation zones may run out. Here we use upslope contributing area as a continuous estimator of the proximity to a ridgeline (defined here as an area with little or no upslope cells) or a valley, in order to assess how hazard may vary with position in the landscape.

Other predictors have been identified in coseismic landslide studies, but these generally have a secondary effect and are not consistently identified as important controls on landslide occurrence (Parker et al., 2017). Elevation and aspect in particular lack a consistent explanation or pattern as a control on coseismic landslide hazard (Parker et al., 2017). Other common predictors are difficult to evaluate 'on the ground' without specialised equipment or knowledge. Soil type (e.g., Lee and Pradhan, 2006), rock type (e.g., Parise and Jibson, 2000), or land cover (e.g., Pradhan, 2013) may be relevant to slope stability but are difficult to identify without specialised training. Curvature (e.g., Xu et al., 2014a) is strongly dependent on the length scale over which it is measured and is extremely difficult to estimate by eye, particularly in rough natural topography. Proximity to roads (e.g., Xu et al., 2012) is often possible to estimate in the field, but inclusion of this factor assumes that all roads are similar in their design, age and construction, and thus have similar impacts on slope stability.

3. Accounting for runout in landslide hazard: reach angle and runout routing

The potential predictors described above are primarily chosen in hazard models for their perceived link to the probability of coseismic landslide initiation. Once triggered, however, landslide material may run out for long distances and over large areas. Thus, there are substantial portions of any landscape where landslide initiation is unlikely but where contact with a landslide is still possible – for example, at the foot of a steep hillslope. Mechanistic modelling of landslide runout is computationally intensive and strongly sensitive to initial conditions, taking it beyond the capacity of exposed communities (e.g., George and Iverson, 2014). In contrast, simple empirical approaches that have shown some predictive power fall into two categories: reach angles and runout routing.

The Fahrboeschung or reach angle from the crown of a landslide to the toe of its deposit has been shown to follow an exponential decrease with landslide volume (Heim, 1882; Corominas, 1996; Hunter and Fell, 2003). The reach angle concept has been incorporated into a small number of hazard maps as a way to represent the probability that a landslide will reach a given location, and

Deleted: ,

Deleted: ,

Deleted: All of the

Formatted: English (United States)

Deleted: linked

Formatted: English (United States)

Deleted: Fahrboschung

Deleted: the

can be coupled with predictions of the probability of landslide initiation (e.g., Kritikos et al., 2015). However, these complex combinations of probability are difficult to distil into a single simple rule and, to our knowledge, this has not yet been done.

If initiation probability is unknown and we make the conservative assumption that any cell can initiate a landslide, then the hazard at a given location becomes proportional to the area that protrudes above a cone with its apex at the location of interest and its sides inclined at a critical reach angle from the horizontal. This approach has similarities with local sloping base level (Jaboyedoff et al., 2004) and excess topography metrics (Blöthe et al., 2015), which both project surfaces through the landscape to identify less stable zones, though neither of these approaches are framed in terms of reach angles. Even this simple approach, which neglects initiation probability, is hard to distil: 1) its conceptual complexity makes it difficult to communicate; 2) its predictions depend on a reach angle parameter that is poorly constrained; and 3) the area protruding from an imaginary surface projected beneath the land surface is very difficult to estimate by eye, particularly in high-relief areas where significant parts of the landscape may be occluded from the viewpoint. An alternative metric would simply be the maximum angle from the horizontal to the skyline, which can be interpreted as the maximum (or worst-case) reach angle for that location. This metric is much simpler and thus easier to communicate and remember, can be estimated by eye, and avoids the problem of choosing a critical reach angle. We choose this as our third potential hazard predictor.

Runout routing approaches assess the probability that landslide debris will reach a given location by assuming that it flows downslope and that its probability of stopping is dependent on some local property of the path along which it flows. This approach ranges in complexity from detailed physics-based treatments (George and Iverson, 2014; von Ruette et al., 2016) to simple empirical rules such as the local slope or junction angle of flowpaths (Benda and Cundy, 1990; Montgomery and Dietrich, 1994; Densmore et al., 1998; Fannin and Wise, 2001). Hazard estimates are then a function of the initiation probability integrated over the upslope area and the stopping probability for each potential event. To incorporate these considerations as simply as possible into a hazard predictor, we introduce a new approach (described below) that accounts for local slope at both the locations of landslide initiation and along the flow path. While this approach does not capture the dynamic

Deleted: .

Deleted: areas

Deleted: Fannin and Wise, 2001;

behaviour of landslide initiation or runout, we include it so that we can test the skill of such non-local approaches and the need to account for them in our simple rules.

4. Earthquake inventories

In this section, we describe the landslide inventories against which we test our four potential predictors. A M_w 6.9 earthquake occurred on 13 October 1993 in the Finisterre Mountains of Papua New Guinea, with a hypocentre at 25 km depth, rupturing the north-dipping Ramu-Markham thrust fault to within a few hundred meters of the surface (Stevens et al., 1998). The event was followed by multiple aftershocks of >M_w 6, including a M_w 6.7 event on 25 October 1993 with a hypocentre at a depth of 30 km. About 4,700 landslides triggered by these earthquakes were mapped from 30 m resolution SPOT images (Meunier et al., 2007). Location accuracy for the landslides is thought to be similar to the pixel size of the satellite images used, ~30 m.

The M_w 6.7 Northridge earthquake occurred in southern California, USA, on 17 January 1994 and ruptured 14 km of a south-dipping blind thrust fault, with a hypocenter at 19 km depth (Wald and Heaton, 1994, Hauksson et al., 1995). The triggered more than 11,000 landslides (Harp and Jibson, 1996). Landslides were mapped immediately after the earthquake using field studies and aerial reconnaissance and were manually digitized on 1:24,000 scale base maps. Landslides >10 m across could be confidently identified and location errors were estimated to be <30 m (Harp and Jibson, 1996).

The M_w 7.6 Chi-Chi earthquake occurred on 21 September 1999 with a hypocentre at 8-10 km depth, rupturing ~100 km of the east-dipping Chelungpu thrust fault in western Taiwan (Shin and Teng, 2001). The earthquake triggered more than 20,000 landslides with the majority occurring across a 3,000 km^2 region (Dadson et al., 2004). Landslides in this region were mapped by the Taiwan National Science and Technology Centre for Disaster Prevention from SPOT satellite images with a resolution of 20 m. Landslides with areas >3,600 m^2 were resolved, resulting in an inventory of 9,272 landslides with location errors estimated to be ~20 m (Dadson et al., 2004).

Deleted: <#> 1994 M_w 6.7 Northridge ¶
Topographic relief and seismicity in southern California are associated with dextral transpression at the Pacific-North America plate boundary (Montgomery, 1993). The study area lies within the western Transverse Ranges of southern California and is largely underlain by weakly cemented sedimentary rocks except for the mainly granitic and gneissic San Gabriel and Verdugo mountains and stronger sedimentary rocks in the Simi Hills (Colburn et al., 1981; Tsutsumi and Yeats, 1999; Parise and Jibson, 2000). Estimated denudation rates for the Santa Monica and San Gabriel mountains are 0.1-1 mm/yr (Meigs et al., 1999; Lave and Burbank, 2004). The region has a warm-summer Mediterranean climate (Peel et al., 2007) with monthly average temperatures ranging from 1 - 18 ˚C (NOAA, 2017) and mean annual precipitation of 0.3–0.9 m (National Atlas of United States, 2011). Vegetation is predominantly annual grassland, sage scrub, and chaparral with some piñon-juniper, oak and pine woodlands (Griffith et al., 2016).¶
The M_w 6.7 Northridge earthquake occurred on 17 January 1994 and ruptured 14 km of a south dipping (35°) blind thrust fault

Moved down [1]: <#> with a hypocenter at 19 km depth (Wald and Heaton, 1994, Hauksson et al., 1995).

Moved down [2]: <#> Landslides were mapped immediately after the earthquake using field studies and aerial reconnaissance and were manually digitized on 1:24,000 scale base maps. Landslides >10 m across could be confidently identified and location errors were estimated to be <30 m (Harp and Jibson, 1996). ¶
¶

Deleted: <#>The earthquake produced recorded ground accelerations of up to 2 *g* (Harp and Jibson, 1996) and maximum surface displacements of ~4 m. More than 11,000 landslides were triggered across a total area of ~10,000 km^2 (Harp and Jibson, 1996).

Deleted: <#>1993 M_w 6.9 Finisterre ¶
Oblique convergence of the Australian and Pacific plates has driven uplift of the Finisterre Mountains to an elevation of ~4 km since 3.7 Ma (Abbott et al., 1997). The Finisterre Mountains consist of volcanic and volcaniclastic rocks thrust over coarse-grained foreland deposits and capped by limestones (Davies et al., 1987; Abbott et al., 1994). Denudation rates in these mountains are up to 0.3 mm/yr averaged over the time of range formation (Abbott et al., 1997). The region has a tropical climate (Peel et al., 2007), with high and stable monthly average temperatures (26-27˚C) and mean annual precipitation ranging from ~2.5 m in the west to ~4 m in the east (Hovius et al., 1998). The vegetation is predominantly tropical wet or tropical montane evergreen forest with sub-alpine grasslands on some of the higher peaks (MacKinnon 1997; Paijmans 1975).¶
A M_w 6.9 earthquake occurred on 13 October 1993,

Deleted: <#>(5 >

Deleted: <#>)

Deleted: <#>with a total surface area of about 55 km^2 were

Deleted: <#>and

Moved (insertion) [1]

Moved (insertion) [2]

Deleted: <#>1999 M_w 7.6 Chi-Chi ¶
Taiwan's mountains are the product of oblique collision between the Philippine Sea plate and the Eurasian continental margin. The study area lies within the central ...

Deleted: <#>–

Deleted: <#> The earthquake produced recorded ground accelerations of up to 1 *g* (Lee et al., 2001) and maximum surface displacements of ~8 m (Chi et al., 2001; Shin and Teng, 2001).

Deleted: <#>; landslides

The M_w 7.9 Wenchuan earthquake occurred on 12 May 2008 with a hypocentre at 14-19 km depth, rupturing ~320 km of the steeply northwest-dipping Yingxiu-Beichuan and Pengguan faults in Sichuan, China (Xu et al., 2009). The earthquake triggered more than 60,000 landslides across a total area of 35,000 km^2 (Gorum et al., 2011; Li et al., 2014). We used a subset of the landslide inventory compiled by Li et al. (2014), who mapped landslides from high-resolution (<15 m) satellite images and air photos. The subset of 18,700 landslides comprises all mapped landslides east of 104° E (Figure S6), and was chosen to avoid gaps in the available 30 m resolution SRTM topographic data. The subset covers a similar range of topographic and lithologic conditions, and experienced a similar range of peak ground accelerations (0.16-1.3 g), to the full inventory (0.12-1.3 g). Location accuracy for landslides is thought to be similar to the pixel size of the satellite images used, ~15 m (Li et al., 2014).

The M_w 7.0 Haiti earthquake occurred on 12 January 2010, with a hypocentre at 13 km depth (Mercier de Lépinay et al., 2011). The complex rupture involved both a blind thrust fault and deep lateral slip on the Enriquillo–Plantain Garden Fault (Hayes et al., 2010, Mercier de Lépinay et al., 2011). The earthquake triggered more than 30,000 landslides across a 3,000 km^2 region (Xu et al., 2014a). We used an inventory of 23,679 landslides mapped by Harp et al. (2016) from publicly available satellite imagery with a resolution of 0.6 m before and after the earthquake; landslides with areas >10 m^2 were resolved (Harp et al., 2017).

The M_w 7.8 Gorkha earthquake occurred on 25 April 2015, rupturing ~140 km of the north-dipping Main Himalayan Thrust in central Nepal (Hayes et al., 2015; Elliott et al., 2016). It had a hypocentre at 8.2 km depth but did not rupture to the surface (Hayes et al., 2015). The event was followed by a series of large aftershocks, including a M_w 7.2 event on 12 May which ruptured a portion of the Main Himalayan Thrust directly east of the 25 April rupture (Avouac et al., 2015). The earthquake triggered approximately 25,000 landslides with a total surface area of about 87 km^2 (Roback et al., 2018). We used an inventory of 24,915 landslides mapped by Roback et al. (2018) from Worldview-2 Worldview-3 and Pleiades imagery, with a resolution of 0.25-0.5 m, before and after the earthquake.

Deleted: <#>2008 M_w 7.9 Wenchuan¶
The Longmen Shan mountain range defines the eastern margin of the Tibetan Plateau with displacement taken up mainly on oblique dextral-thrust faults (Burchfiel et al., 1995; Densmore et al., 2007). The Longmen Shan are underlain by a complex lithological assemblage comprising Proterozoic granitic massifs, a Palaeozoic passive margin sequence, a thick Triassic-Eocene foreland basin succession, and minor exposures of poorly-consolidated Cenozoic sediment (Burchfiel et al., 1995). Denudation rates are estimated at ~0.5 mm/yr over decadal to millennial timescales (Ouimet et al., 2009; Godard et al., 2010; Liu-Zeng et al., 2011). The region has a humid subtropical climate (Peel et al., 2007), with an annual average temperature of 15-17 °C and average annual rainfall varying from ~1100 mm at the margin to ~600 mm on the plateau, of which 70%–80% falls from June to September (Liu-Zeng et al., 2011; Li et al., 2016). The natural vegetation is montane broad-leaved and conifer forest below 4000 m with alpine shrub land and steppe vegetation at higher elevations (Yu et al., 2001).¶

Deleted: <#>2009). It had an oblique dextral-thrust focal mechanism with a hypocentre at 14-19 km depth. The earthquake produced recorded ground accelerations of up to 1 *g* (Li et al., 2008) and maximum vertical and dextral displacements of 6.2 m and 4.5 m, respectively (Liu-Zeng et al., 2009; Gorum et al., 2011

Deleted: <#>(

Deleted: <#>),

Deleted: <#>2010 M_w 7.0 Haiti¶
Haiti's mountains are the product of oblique convergence between the Caribbean and North American plates (Pubellier et al., 2000). The study area is underlain by northwest-southeast oriented sub-parallel belts of igneous, metamorphic and sedimentary rocks (Sen et al., 1988, Escuder-Viruete et al., 2007). Mean elevation and relief generally increase from north to south, to a plateau at ~2500 m (Gorum et al., 2013). The region has a tropical climate (Peel et al., 2007) with a mean annual temperature of 25˚C and mean annual precipitation of ~1.2 m, with two rainy seasons per year (April-June and October-November) and hurricanes between June and November (Gorum et al., 2013; Libohova et al., 2017). The study area lies predominantly within the moist broadleaf forest biome with some pine or dry broadleaf forest (Olsen et al., 2001) but also has extensive (~50% by area) savannah, shrub or herbaceous cover (Churches et al., 2014).¶

Deleted: <#>but without any detectable surface rupture

Deleted: <#>the Léogâne

Deleted: <#>, responsible for ~80% of the seismic moment (Hayes et al., 2010) as well as

Deleted: <#>2014

Deleted: <#>

Deleted: <#>2015 M_w 7.8 Gorkha¶
The Himalayas are the product of active continental convergence of India and Asia, much of which is accommodated by the seismogenic Main Himalayan Thrust (Lavé and Avouac, 2000). The study area is underlain by variably metamorphosed sedimentary and igneous rocks of Proterozoic and early Paleozoic age with Paleozoic and Mesozoic sedimentary rocks and low-grade metasedimentary rocks to the north marking the southern margin of the Tibetan Plateau (Hodges et al., 1996; Searle and Godin, 2003; Craddock et al., 2007). Denudation rates in the study area range from 0.3-3 mm/yr over millennial time scales (Lupker et al., 2012; Godard et al., 2014). Mean annual temperature varies with elevation across the study ...

Deleted: <#>2017

Deleted: <#>2017

Deleted: <#><

These epicentral areas encompass a large range of millennial scale erosion rates (0.1 to >7 mm yr^{-1}), lithological properties (metamorphic, igneous and sedimentary), climatic conditions (Mediterranean to tropical) and vegetation covers (chapral, savannah, tundra, tropical and subtropical forest); see table S2 and Figures S3 to S8 in Supplementary Information. We choose this range of settings in order to test the general applicability of any rules that we can extract.

5. Methods

5.1. Conditional probability and landslide hazard

Landslide hazard can be defined as the probability of being hit by a landslide in a given location and within a given time interval (Lee and Jones, 2004). Here we make no distinction between the consequences of being hit by landslides of different sizes or velocities, assuming that all are equally dangerous. This probability can be expressed mathematically as $P(L|x,y,t)$, where L is the outcome of being hit by a landslide, x,y are the coordinates for a particular location, and t is the time interval of interest. We do not address the timing of landsliding, assuming that this is driven by the timing of an earthquake and is thus unpredictable (Geller, 1997). Instead we focus on landslide susceptibility given an earthquake that produces shaking of unknown intensity at a location (x,y), hence the notation $P(L|x,y)$. We assume that the hazard at that location can be approximated by some location-specific characteristic (a). Thus, the landslide hazard at (x,y) is the conditional probability of being touched by a landslide given the value of the characteristic at that location, $P(L|a)$, and can be calculated using Bayes' Theorem:

$$P(L|a) = \frac{P(L)\,P(a|L)}{P(a)} \qquad (1)$$

where a is a specific characteristic of the location, such as the topographic slope. If we assume that the relationships between past landslides and local characteristics are good predictors of their future relationships then we can construct empirical conditional probability calculations from landslide inventories. This approach has proved successful for a range of applications, including identifying topographic controls on vegetation patterns (Milledge et al., 2012) and the rainfall conditions that

Deleted: window

Formatted: Font: Italic

Formatted: Font: Italic

Formatted: Font: Italic

Formatted: Font: Italic

Deleted: window

Formatted: Font: Italic

Formatted: Font: Italic

Formatted: Font: Italic

Formatted: Font: Italic

Deleted: Bayes

Deleted: (e.g.,

Deleted:).

Deleted: If we grid the topography, then the Bayes trigger landslides (Berti et al., 2012). If we grid the topography, then the Bayes' equation can be easily rewritten in terms of the numbers of grid cells, and in this form the direct equivalence of landslide conditional probability and landslide area density (e.g., Meunier et al., 2007; Dai et al., 2011; Gorum et al., 2014) is clear:

$$P(L|a) = \frac{N(a \cap L)}{N(a)} \tag{2}$$

where $N(a \cap L)$ is the number of cells with a given value of characteristic a that are touched by a mapped landslide, $N(a)$ is the number of cells with the characteristic of a in the entire study area, and the study area is defined by the smallest convex hull that contains all of the observed landslides. To account for variability in the magnitude of shaking between the six study areas, we normalise the conditional probability of being hit by a landslide $P(L|a)$ by the study area average probability of landsliding $P(L)$ to generate a relative hazard. This can be shown to be directly equivalent to the 'frequency ratio' (e.g., Lee and Pradhan, 2007; Lee and Sambath, 2006; Yilmaz, 2009; Kritikos et al., 2015):

$$\frac{P(L|a)}{P(L)} = \frac{N(a \cap L)/N(a)}{N(L)/N(S)} = \frac{N(a \cap L)}{N(a)}\frac{N(S)}{N(L)} \tag{3}$$

where $N(S)$ is the total number of cells in the study area and $N(L)$ is the number of cells touched by landslides. Our normalised conditional probability is also directly equivalent to the 'probability ratio' used by Lin et al. (2008) and Meunier et al. (2008) since, from Bayes' Theorem:

$$\frac{P(L|a)}{P(L)} = \frac{P(L)\,P(a|L)}{P(a)P(L)} = \frac{P(a|L)}{P(a)} \tag{4}$$

We display the normalised conditional probability on a logarithmic scale for readability, resulting in a probability metric that is strongly similar to the 'information value' metric used in some landslide susceptibility analyses (e.g., Yin and Yan, 1988). We evaluate both one-dimensional conditional

Formatted: Font: Italic

Formatted: Font: Italic

Formatted: Font: Italic

Formatted: Font: Italic

Formatted: Font: Italic

Formatted: Font: Italic

Deleted: Bayes

probability in terms of one predictor variable a, and two-dimensional conditional probability in terms of two predictors considered jointly.

Conditional probability analysis is advantageous for its direct link to hazard and does not require us to impose a functional form to the data. However, the results are partly dependent on bin size and location for the predictor variable, and bins with few observations (i.e., those for which $N(a) << N(S)$) can result in noisy data that are difficult to interpret. We use the approach of Rault et al. (2018) to identify the parts of the conditional probability data where our observations are sparse, leading to lower confidence in the results. We compute the confidence interval I_p associated with the random drawing of the *N(L)* landslide cells from the landscape distribution of the predictor variable. If the normalised conditional probability $P(L|a) / P(L)$ is within the interval I_p then we cannot exclude the possibility that the difference between the conditional and study area average probabilities is simply the result of random fluctuations. Given that landslides are rare events even in these large earthquakes, we assume that landslides are independent and can be modelled with Bernoulli sampling. Since the binomial distribution is well approximated by a normal distribution when samples sizes are large (i.e. N(L) > 30) and in the absence of extreme skew (i.e. $N(L) \times (P(a|L) > 5$ and $N(L) \times (1 - (P(a|L)) > 5)$, then the 90% confidence interval can be estimated as:

$$I_p = \left[1 - 1.96\sqrt{\frac{1-P(a|L)}{N(L)\,P(a|L)}};\, 1 + 1.96\sqrt{\frac{1-P(a|L)}{N(L)\,P(a|L)}};\right] \qquad (5)$$

We distinguish conditional probability values that exceed this confidence interval I_p in the analysis below.

To aid interpretation in the two-dimensional case, we also perform a two-variable logistic regression with both local slope and upslope contributing area as predictors. Whilst other statistical approaches could be used here (e.g. Pradhan, 2013), our intention is not to find the statistical approach that provides the most powerful synthesis of the different variables, but to test the effectiveness of the variables themselves at distinguishing hazard when applied in the form of simple rules.

5.2. Receiver operating characteristic curves

Any simple rule for identifying more or less hazardous locations in the landscape will produce a relative measure of landslide probability. To evaluate this measure against a binary landslide map

Deleted: .

Deleted:)<<

Formatted: Font: Italic

Formatted: Font: Italic

Deleted: To aid interpretation in

Deleted: presence

Deleted: noise, we fit cubic polynomial functions

Deleted: one-dimensional

Deleted: and a logistic function to two-dimensional data. To highlight the parts of the data where we have few

Deleted: and thus where our

Deleted: is lower, in the one-dimensional case we include a single bulk PDF

Deleted: on

Deleted: x-axis below the

Deleted: curve,

Deleted: we limit ourselves to calculating

Deleted: only where there are more than 10 observations per bin

Deleted: dimensional case

or inventory (where every cell is classified as landslide or non-landslide), it must be converted into a binary classification. A common approach to this problem is to construct a receiver operating characteristic (ROC) curve (e.g., Frattini et al., 2010). This curve quantifies both the benefit of a given classification in terms of successfully classified outcomes (landslide and non-landslide locations correctly identified, representing true positive and true negative outcomes, respectively) and also the cost (non-landslides identified as landslides, known as false positives; and vice versa, known as false negatives). The ROC curve is constructed by thresholding a continuous variable (e.g., slope) and calculating the true positive rate as the number of true positives normalised by all positive observations, and the false positive rate as the number of false positives normalised by all negative observations. Evaluation of these rates at different threshold values results in a curve, where the 1:1 line reflects the naïve random case. The area under the curve (AUC) tends to 1 as the skill of the classifier improves towards perfect classification and to 0.5 as the classifier worsens towards the naïve case. We calculate ROC curves for all of our chosen predictive approaches for each inventory.

5.3. Topographic analysis

All of the metrics tested here are defined using topographic data in the form of digital elevation models (DEMs). We use 30 m resolution DEM data drawn from the most widely-used, freely-available source for each site: for Northridge they are derived from down-sampled 10 m NED elevation data (https://lta.cr.usgs.gov/NED), while for all other sites we use 1-arc sec Shuttle Radar Topography Mission (STRM) elevation data (http://srtm.csi.cgiar.org/).

5.3.1. Slope and upslope contributing area

We calculate local slope as the steepest path to a downslope neighbour from each cell (Travis et al., 1975) because calculating slope over larger (e.g., 3 x 3 cell) windows for a 30 m resolution DEM results in considerable underestimation (Claessens et al., 2005). We calculate upslope contributing area using a multiple flow direction algorithm (Quinn et al., 1991) having filled pits using a flood fill algorithm (Schwanghart and Kuhn, 2010), and normalising by the grid cell width to minimise grid

Deleted: positives
Deleted: negatives
Deleted: (i.e.
Deleted:)
Deleted: (random)
Deleted: at all sites
Deleted: the
Deleted: . 3x3
Deleted:).

resolution biases. These topographic analyses are performed in Matlab using TopoToolbox v1.06 (Schwanghart and Kuhn, 2010).

5.3.2. Skyline angle analysis

To capture the effects of both landslide initiation and runout, we define the skyline angle as the maximum angle from horizontal to the skyline for a given location. This metric is easily estimated by eye in the field, and gives a worst-case reach angle for the location of interest, but is runout-dominated in that it does not take into account the probability of initiation.

For each cell in a study area, we estimate the skyline angle by calculating vertical angles between the target cell and every other cell within a 4.5 km radius. This search radius is chosen to greatly exceed the average hillslope lengths in all study areas and thus to fully capture the local skyline. The longest average hillslope length out of our study areas is ~500 m for Wenchuan, estimated following the method of Roering et al. (2007). We choose a search radius nine times larger than this hillslope length to ensure redundancy in capturing the local skyline and because the only disadvantage of a larger radius is increased computational cost. This approach is physically limited in at least two ways (Figure 1a). First, it does not account for the dependence of runout on the size of the initial failure or on increases or decreases of failure volume during runout (e.g., Corominas, 1996). Second, it does not honour potential material flow paths. That is, the skyline cell that generates the steepest slope to the target cell may not be connected to the target cell by a flowpath with monotonically decreasing elevation. However, this metric provides a measure of the gravitational potential energy available to drive runout in the vicinity of the target cell.

Deleted: effect

Deleted: can be interpreted as the maximum (or

Deleted:)

Deleted: that

Deleted: . It

Deleted: a

Deleted: metric

Deleted: dominant channel spacing for the

Deleted: area with widest spacing (Wenchuan)

Deleted: For the Wenchuan study area the characteristic

Deleted:), is ~500 m. Thus a conservative estimate on dominant channel spacing would be ~1 km.

Deleted: window size

Deleted: skyline angle estimates become asymptotically insensitive to window size, so that

Deleted: constraint

Deleted: run time. MATLAB code for the routine is included in the supplemental information

Deleted: how the

Deleted: may increase or decrease

Deleted: .

Deleted: The

Deleted: does

Deleted: have to

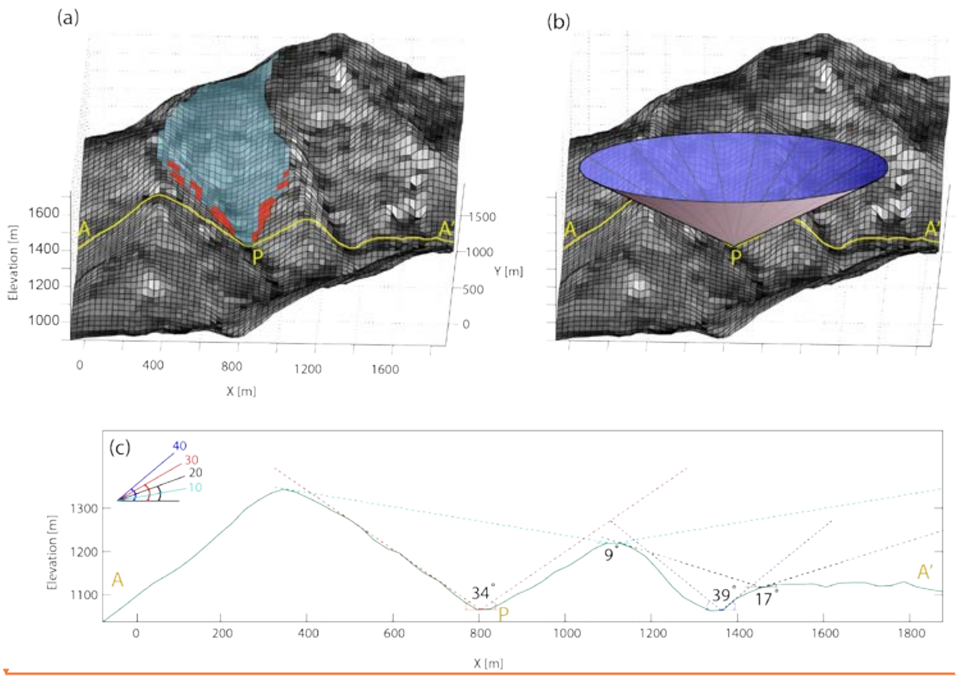

Figure 1. Schematic view of the different topographic metrics tested here. (a) perspective view of a landscape with each cell shaded according to its local slope from light (steep) to dark (gentle). The upslope contributing area for point P is coloured blue, and the cells steeper than 40˚ that have a flow path to P that is never less than 10˚ are coloured red. (b) the same perspective view with a cone projected from point P at an angle of 34˚ so that the surface of the cone is in places tangent to but never intersects the ground surface, indicating a maximum skyline angle of 34˚ for point P. (c) cross section A-A' through the landscape (highlighted in yellow on panels a and b) with dashed lines showing skyline angles at four example locations.

5.3.3. Runout routing analysis

To assess the importance of non-local runout paths on landslide probability, we follow the approach of Dietrich and Sitar (1997) who proposed the simplest possible debris flow runout model, requiring only thresholds to define the initial instability and for downslope motion to continue. This simple model, referred to as SHALRUN, has been integrated with the coupled hydrologic-slope stability model SHALSTAB in an efficient parallel framework to predict landslide hazard potential in California

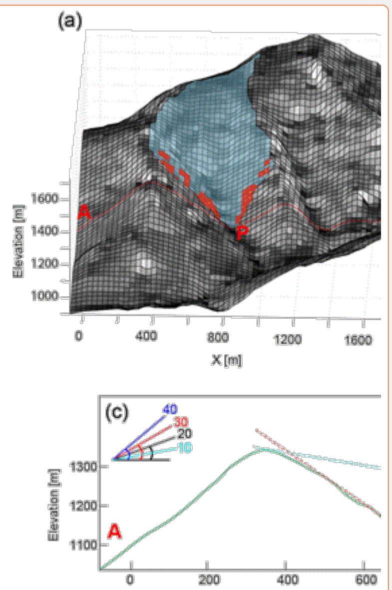

Deleted:

Deleted:),

Deleted: 39˚

Deleted:),

Deleted: A

Deleted:),

Deleted: red

Deleted: was

(Bellugi et al, 2011). SHALRUN requires only two field-calibrated parameters: a critical rainfall threshold to define instability, and a minimum slope threshold for downslope motion to continue. To apply this model in the context of coseismic landslides, we modify the condition for landslide initiation, replacing the critical rainfall threshold with a slope threshold, to create a new model that we refer to as SHALRUN-EQ. We thus assume that landslide initiation and deposition are entirely dependent on the local slope of the ground surface - that is, landslides are more likely to initiate on steeper slopes and deposit on flatter slopes. More formally, SHALRUN-EQ predicts the upslope hazard area A_h as the upslope area weighted by the joint probability of landslide initiation and runout. Locations with higher A_h should have higher exposure to coseismic landslide hazard than those with low (or no) A_h. Formulation of the model requires: (1) determination of the mobilisation probability P_{mi} at each cell i in the study area; (2) determination of the connection probability P_{cij} for mobilised material from each cell i to the target cell j; (3) convolution of (1) and (2) to get the locational hazard P_{mcij}; and (4) accumulation of the locational hazard to determine a hazard area A_{hj} above each target cell j.

In order to generate a simple rule, our model assumes that landslide initiation and deposition are entirely dependent on the local slope of the ground surface θ. For landslide initiation, we assume that locations steeper than a threshold slope θ_m are all equally capable of initiating a landslide with probability P_{mi}:

$$P_{mi} = \begin{cases} 1: \ \theta_i \geq \theta_m \\ 0: \ \theta_i < \theta_m \end{cases} \qquad (6)$$

where θ_i is the observed local slope in a downslope direction at cell i and θ_m is the threshold slope required for landslide initiation.

In order to represent a landslide hazard, mobilised material must be able to run out from the initiation point i to the target cell j. This relationship is binary: either these points are connected by a viable runout path or they are not. We define flow paths using multiple flow routing to all downslope cells weighted by the slope of the flow path (Quinn et al., 1991). This path must enable continued runout for its entire length; if at any point on the flow path the material is fully deposited, then that initiation

Deleted: required
Deleted: (SHALRUN-EQ)
Deleted: .
Deleted: θ (i.e.,
Deleted:), further increasing the simplicity of the model
Formatted: Font: Italic
Formatted: Font: Italic
Formatted: Font: Italic
Deleted: (P_{mi});
Deleted: (P_{cij});
Deleted: (
Deleted:);
Deleted: (A_{hj}).
Deleted: θ (i.e. landslides are more likely to initiate on steeper slopes and deposit on flatter slopes).
Deleted: slopes above
Deleted: (5
Deleted: critical
Deleted: runout
Deleted: We assume that the flow path will follow the path of steepest descent.

zone will be disconnected from the target cell j. Surface slope has previously been used to describe the probability that landslide material entering a cell will be deposited rather than continuing into the next downslope cell (e.g., Benda and Cundy, 1990; Fannin and Wise, 2001). For landslide deposition, we apply the simplest possible stopping condition, and assume that landslide runout ceases on slopes gentler than a critical angle (θ_s). The probability that a landslide initiated at cell i reaches the target cell j (P_{cij}) can thus be expressed as:

$$Pc_{ij} = \begin{cases} 1: \theta min_{ij} \geq \theta_s \\ 0: \theta min_{ij} < \theta_s \end{cases} \qquad (7)$$

where θmin_{ij} is the minimum slope along the flow path from cell i to cell j, and θ_s is the critical slope required for stopping. We recognise that this simple stopping condition would be violated for landslides large enough to continue beyond the first cell with angle below the deposition threshold and discuss the implications of this simplification in Section 7.1.

We combine the initiation and runout probabilities to calculate the locational hazard P_{mcij} as the area a_i of cell i weighted by the probability that a landslide is both mobilised in cell i and is connected to cell j:

$$P_{mcij} = a_i \, P_{mi} \; P_{cij} \qquad (8)$$

Assuming that θ_s > 0, we calculate the hazard area A_{hj} for each target cell j by summing locational hazard in the n cells upslope of j, normalised by grid cell width to minimise grid resolution bias:

$$A_{hj} = \sum_{i=1}^{n} \left(\frac{a_i}{l_j} \, P_{mi} \; P_{cij} \right) \qquad (9)$$

where l_j is the grid cell width (30 m). Equation 9 is evaluated for every cell in the study area to generate a spatial grid of hazard area A_h (Figure 2). Our choice of step functions for the mobilisation (P_{mi}) and connection (P_{ci}) probabilities allows us to interpret A_h as the upslope area with slope steeper

Deleted: cell j. Thus, the point along a given flow path that is most likely to cause deposition becomes the controlling location for the connection of all upslope points. Surface slope has

Deleted: run-out

Deleted: point

Deleted: point

Deleted: (6

Deleted: for

Deleted: (

Formatted: Font: Italic

Deleted:) in

Deleted: (7

Deleted: Assuming that θ_s >

Formatted: Font: Italic

Deleted: the unit contour length

Deleted: 8

Deleted: unit contour length at *j*, calculated as $a_j^{0.5}$.

Deleted: 8

Deleted: P_m

Deleted: P_c

Deleted: per unit contour width

Deleted: local

than θ_m from which landslide debris can reach the target cell without passing over a slope of gentler than θ_s. Alternative formulations could be used for P_{mi} and P_{ci} but these would result in a less intuitive index that would be difficult to implement as a simple rule.

There is implicit resolution dependence to the stopping condition θ_s because it assumes that the low gradient area is long enough (in terms of flow path length) that the landslide will stop. Similarly, there is resolution dependence to the initiating condition θ_m as topographic surfaces will be more or less smooth, depending on the resolution of the DEM (Claessens et al., 2005). Also, the initiation probability is based on local slope alone and so does not account for any of the other possible drivers of coseismic landslide initiation, such as topographic amplification (Meunier et al., 2008) or pore water pressure (e.g., Xu et al., 2012). While many more complex models exist that account for initiation volumes and flow dynamics (e.g., George and Iverson, 2014; von Ruette et al., 2016), we seek the simplest possible model that captures the effects of drainage networks in accumulating hazard, of steep slopes in landslide initiation, and of gentle slopes in landslide deposition.

The model has two parameters (θ_m and θ_s), both of which are effective rather than measurable. We first optimise the model for each inventory to establish its performance under the best possible scenario, finding the values of θ_m and θ_s that provide the best fit to the inventory data. We then test the model using the average of the optimised parameters from the six inventories, in order to represent a more realistic application where these parameters must be estimated from previous earthquakes. Thus, the values of θ_m and θ_s should not be interpreted as mechanistic thresholds, but rather as the result of an optimisation that also depends on the DEM resolution.

Deleted: a
Formatted: Font: Italic
Deleted: will
Deleted: interest by moving downslope along a path that is always steeper
Deleted: P_m
Deleted: P_c
Deleted: since
Deleted: Classens
Deleted:),
Deleted: where
Deleted: model is fitted
Deleted: events
Deleted: optimization

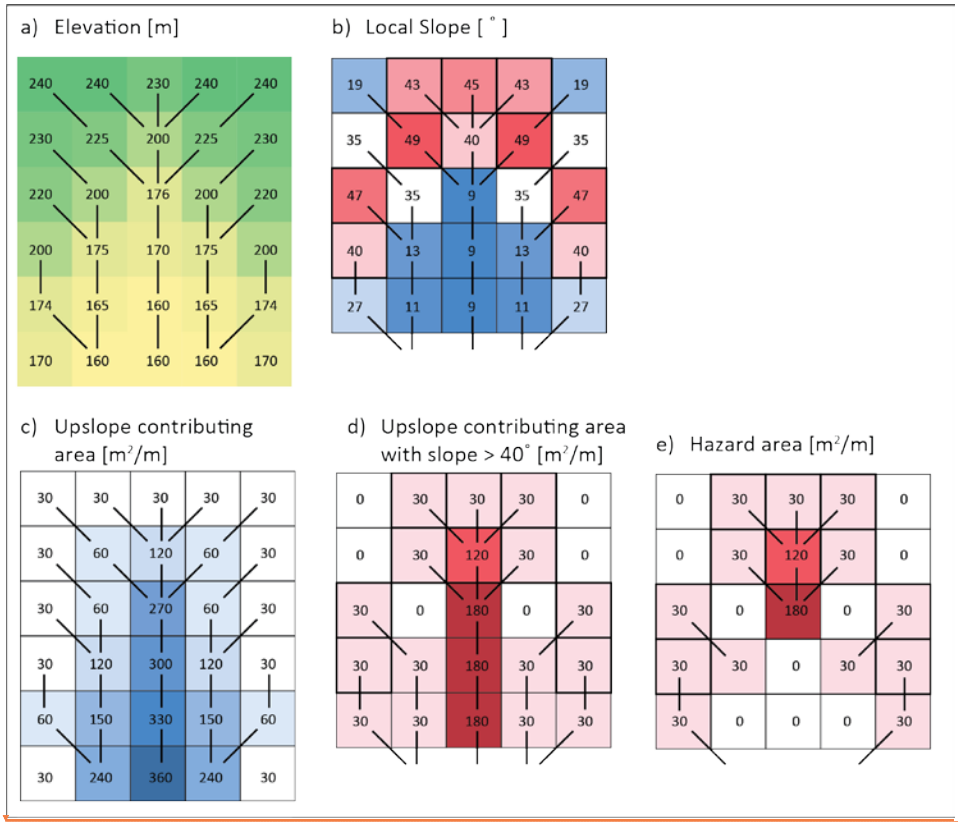

Figure 2. SHALRUN-EQ hazard area calculations for a simplified (steepest flowpath) example with an initiation angle of 40˚ and a stopping angle of 10˚; a) elevations from a 30 m resolution digital elevation model for an area of topographic convergence, where lines show flow paths from cell to cell; b) local slope with thick outlines showing cells steeper than 40˚; c) upslope contributing area; d) upslope contributing area steeper than 40˚; and e) hazard area, the upslope area steeper than 40˚ with flow paths that do not fall below 10˚.

Deleted:

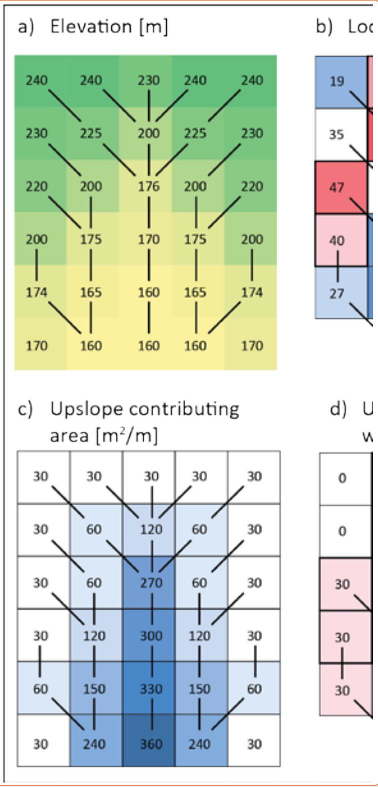

Deleted: Worked example of

Deleted: 39˚

Deleted: .

Deleted:),

Deleted: . Lines

Deleted: steepest flowpaths

Deleted: .

Deleted:),

Deleted: calculated as the steepest path to a downslope neighbour. Thick

Deleted: show

Deleted: 38˚.

Deleted:),

Deleted: using steepest flow path routing.

Deleted:),

Deleted: 38˚.

Deleted:),

Deleted: defined as

Deleted: 38˚

6. Results

6.1. Local slope

For all inventories, landslide hazard increases as an approximately exponential function of local slope (Figure 3a). This behaviour is consistent up to slopes of 70˚, beyond which small sample sizes limit our confidence. Conditional probability exceeds the study area average landslide probability for slopes >30-35 in four of the inventories, and for slopes >20-25 for the remaining two (Northridge and Haiti). This suggests that slopes <30˚ are generally safer than average, while those >45˚ have a landslide hazard >200% of the average, and those >50˚ are generally >300% of the average. The conditional probability curves for Finisterre, Chi-Chi and Gorkha largely collapse on each other when normalised by study-area average probability (Figure 3a). However, landslide hazard is less sensitive to slope for Wenchuan and more sensitive for Northridge and Haiti. This variability between inventories may be a result of weaker rock strength in the Northridge and Haiti study areas. When local slope is normalised by study area average slope (Figure 3b), the curves collapse onto those from the other study areas. Comparing the combined PDF of study area slopes (Figure 3a) with the hazard curves indicates that the majority of landslide hazard is concentrated in a small subset of each study area (that is, on slopes >35˚). This implies that 1) many of the modest (<15˚) slopes on which people in these areas generally choose to live are exposed to relatively low hazard (less than half the study area average for all but Wenchuan); and 2) any choice to spend time or build infrastructure on steeper slopes should take into account the considerable associated increase in exposure to coseismic landslide hazard.

Deleted: probability
Deleted: For four of the six inventories, conditional
Deleted: steeper than
Deleted: 35˚, with
Deleted: lower at 20˚ and 25˚.
Deleted: probability
Deleted: The
Deleted: likely reflects specific study area properties such as the more dissected topography within
Deleted: amalgamated
Deleted: conditional probability
Deleted: the
Deleted: burden is held by the minority
Deleted: recognise

6.2. Upslope contributing area

For all inventories, landslide hazard increases from less than the study area average at the lowest upslope contributing areas – that is, at the ridge tops – to a peak or plateau at intermediate upslope contributing areas (Figure 3c). Locations with the lowest upslope contributing area also have the lowest hazard for four of the six inventories, with Northridge and Finisterre as exceptions. For Northridge, the zone of lower than average hazard extends only to upslope contributing areas of ~40 m^2/m; for Finisterre it extends to ~100 m^2/m, for Chi-Chi and Haiti to ~150 m^2/m, and for Wenchuan and Nepal to ~200 m^2/m. The location of peak landslide hazard broadly coincides with the inflection

Deleted: probability
Deleted: below
Deleted: , from which it declines in four of the six inventories
Deleted: 3b
Deleted: landslide probability
Deleted: landslide probability
Deleted: probability

in average slope for a given upslope contributing area (Figure 4). This inflection is commonly used as an indicator of the transition from hillslopes to rivers (Montgomery and Foufoula-Georgiou, 1993; Stock and Dietrich, 2006; Hancock and Evans, 2006), suggesting that maximum (or near-maximum) landslide hazard occurs at the transition from hillslopes to channels (Figure 3c). We use this inflection to identify a reference upslope contributing area associated with channel initiation for each landscape. Normalising upslope contributing area by this reference area shifts the conditional probability curves laterally, aligning the Northridge curve with those from the other sites (Figure 3d). This normalised analysis shows that landslide hazard is highest within low-order channels, where upslope contributing areas are less than ten times the upslope contributing area associated with channel initiation in the study sites (Figure 3d). Further downstream, landslide hazard generally decreases with increasing upslope contributing area although limited sample sizes mean that we cannot confidently interpret the curves beyond ~1000 m^2/m.

Deleted: inflexion

Deleted:

Deleted: probability

Deleted: 3b). Landslide probability

Deleted: this transition point for four of the six inventories, gently for Finisterre and Chi-Chi, more steeply for Northridge and Haiti, and in all cases with an increase in scatter that is likely due to the small number of observations with upslope contributing area >

Deleted:

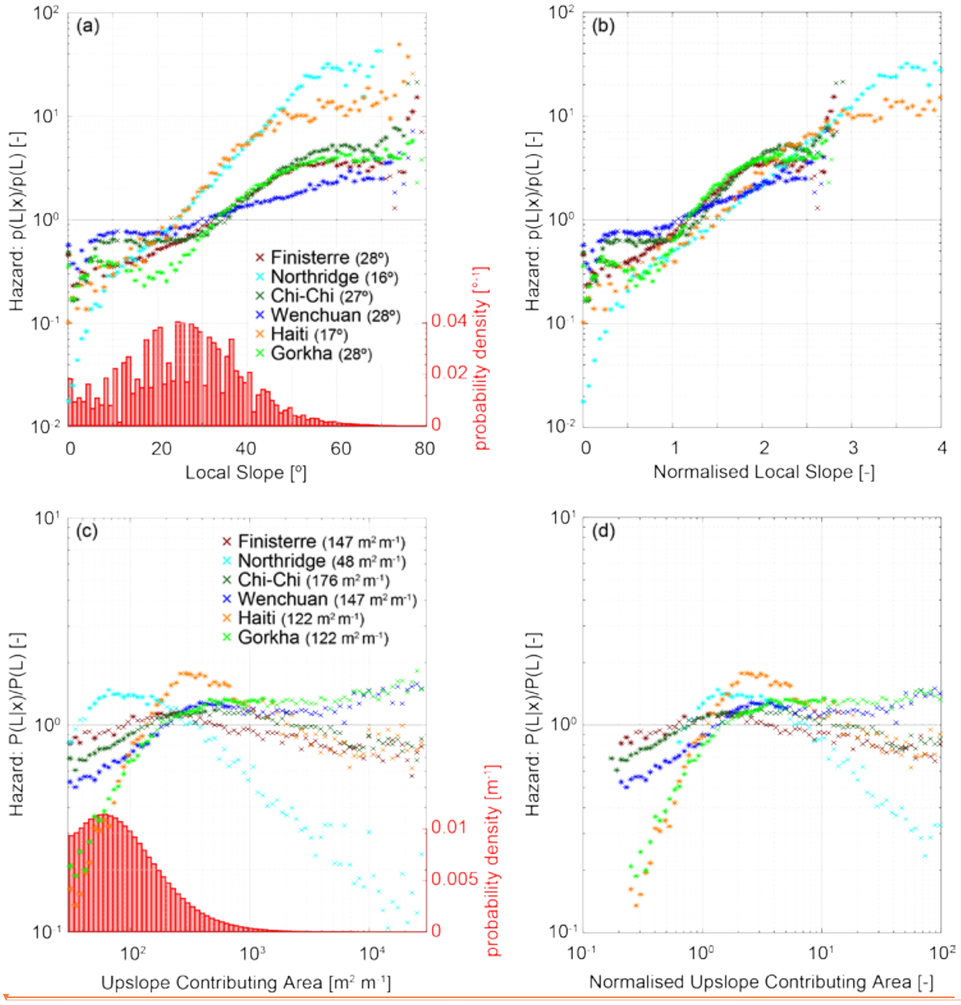

Figure 3. Landslide hazard defined as conditional probability $P(L|x)$ normalised by study area average landslide probability $P(L)$, where x is a) local slope; b) local slope normalised by the study area average slope; c) upslope contributing area per unit cell width; and d) upslope contributing area normalised by the upslope contributing area of the inflection in average slope. Solid black lines show normalised probability of 1, the study area average; thus, points above this line have above-average landslide hazard compared to the study area as a whole. Asterisks indicate values for which conditional probability differs from the study area average probability at 90% confidence. Red bars in (a) and (c) show histograms of local slope and upslope contributing area over the six inventories.

Deleted:

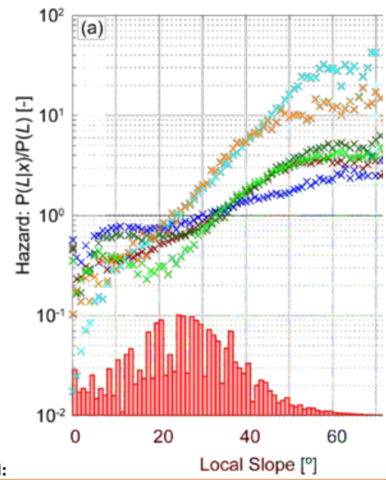

Formatted: Font: Italic

Deleted: and b

Formatted: Font: Italic

Deleted: contour length. Red bars show histograms of each variable over the six inventories. Note logarithmic y-axes and different y-axis scales in panels a and b. The solid

Deleted: a

Deleted: equivalent to

Deleted: the solid black

Deleted: greater than

Deleted: . Legend includes study

Deleted: average landslide probabilities for each inventory (

Numbers in brackets show study-area average slopes in panel (a), and upslope contributing area at the hillslope-channel transition in panel (c).

6.3. Local slope and upslope contributing area combined

When slope and upslope contributing area are examined in combination, the highest landslide hazard is consistently found at the highest upslope contributing area for a given slope, or the highest slope for a given upslope contributing area (Figure 4). In this case normalisation adds little to our understanding of the relationship between landslide hazard and the two metrics under consideration, with normalised results shown in Figure S9 for reference.

Two-dimensional conditional probability analysis is sensitive to the sample size within each bin, limiting our confidence in the results for large parts of the slope-upslope contributing area space. The logistic regression contours do not suffer the same limitation, however, and provide important additional information on the form of the relationship between landslide hazard, slope and upslope contributing area. Taken together, the logistic regression contours and conditional probability surfaces show that the lowest hazard is consistently found at locations with both low slope and low upslope contributing area. Importantly, landslide hazard increases more steeply with increasing slope than with increasing upslope contributing area, indicating the dominance of local slope in setting landslide hazard. There is some variability in the orientation of the hazard contours between inventories, with Finisterre and Northridge showing the strongest slope dependence and Wenchuan showing the strongest upslope contributing area dependence (Figure 4).

The shape of the two-dimensional probability surface determines the best course of action in terms of choosing alternative locations for a particular asset or activity, but such action is also constrained by what is possible. The average slopes for each upslope contributing area (shown by the dashed lines in Figure 4) indicate that for Northridge, Finisterre, Chichi, and Haiti there are rarely situations where a reduction in upslope contributing area will not involve (on average) an increase in slope that will actually increase landslide hazard. However, for locations in Wenchuan and Gorkha with upslope contributing areas of 300 to 10,000 m^2/m, the hazard reduction due to reducing upslope contributing area is not offset by the associated increase in slope. This suggests that, for the former inventories, it is always beneficial to decrease slope even at the expense of upslope contributing area, while for

Deleted:).

Deleted: probability

Deleted: The lowest probabilities are found at locations with both low slope and

Deleted: cells with very low slopes have low landslide probability almost independently of

Deleted: probability

Deleted: probability. This dominance

Deleted: also reflected

Deleted: probability

Deleted: derived from logistic regression. There is variability in contour orientations

Deleted: ¶

Deleted: slope

Deleted: line

Deleted: indicates

Deleted: ,

Deleted: probability

Deleted: area

Deleted: probability

the latter inventories benefit is more dependent on initial location. In general, the average slope contour appears to separate higher and lower than average landslide hazard in slope-upslope contributing area space, suggesting that higher than average landslide hazard is consistently found on higher than average slopes for a given upslope contributing area.

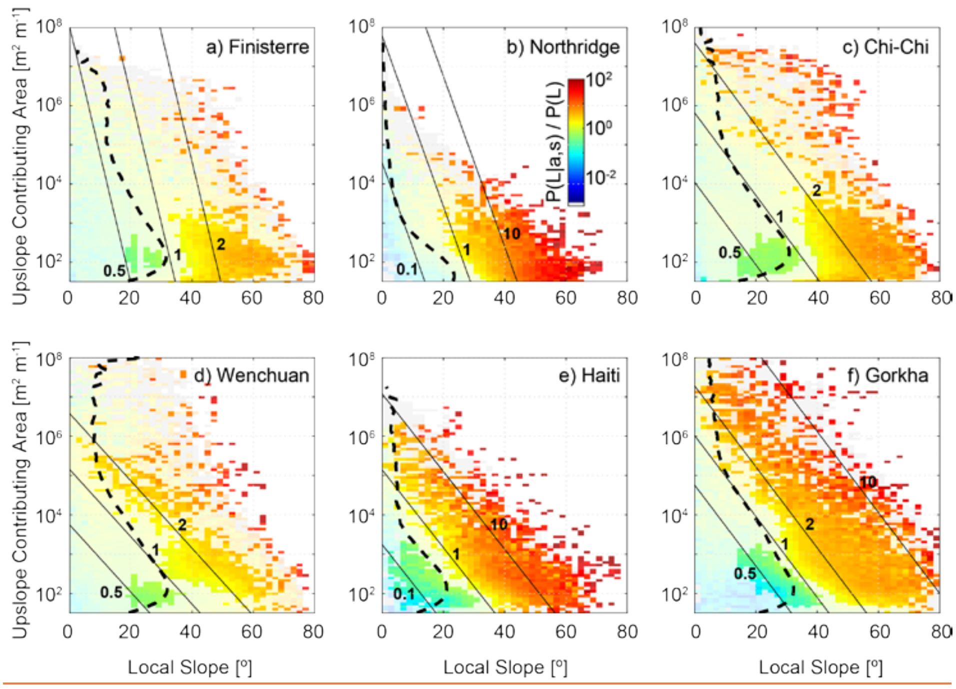

Figure 4. Two-dimensional plots of landslide hazard defined as conditional landslide probability *P*(*L*|*s*,*a*) normalised by study area average landslide probability *P*(*L*), where s is local slope and a is upslope contributing area per unit cell width. Dashed lines show the mean slope per upslope contributing area bin, using 100 logarithmically-spaced bins. Solid lines are landslide probability contours derived from logistic regression in the same units as the conditional landslide probability surface. Grey cells indicate slope-area pairs with data but with no cells touching a landslide. Note that upslope contributing area is shown on a logarithmic axis, so that maintaining a constant landslide probability for a given increase in slope requires a larger reduction in upslope contributing area at

Deleted: it

Deleted: probability

Deleted: probability

Deleted: always

Deleted: Page Break

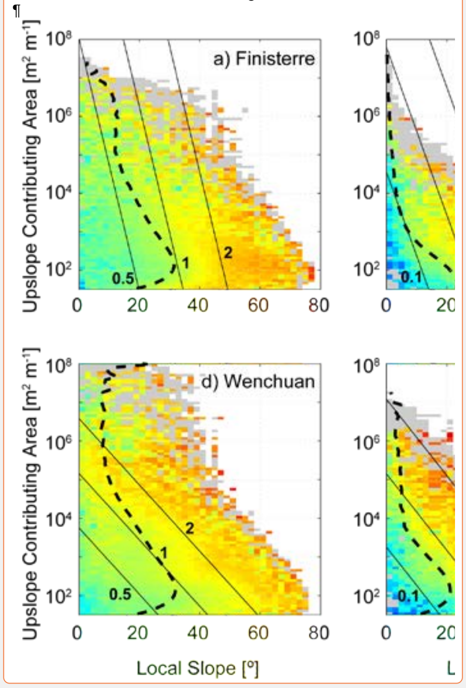

Deleted: ,

Formatted: Font: Italic

Formatted: Font: Italic

Deleted: contour length.

Deleted: relative hazard

Deleted: relative hazard

low slopes than at high slopes. Fainter colours indicate landslide hazard estimates that do not differ significantly from the study area average at 90% confidence.

6.4. Skyline angle

Landslide hazard increases as an approximately exponential function of maximum skyline angle (Figure 5a), similar to the relationship with local slope (Figure 3a). We are confident in this behaviour for skyline angles in the range 5° to 70°, outside of which small sample sizes limit our confidence. Landslide hazard exceeds the study area average at skyline angles ≥ 27-28° for Northridge and Haiti, 34° for Wenchuan, and 38-40° for Finisterre, Chi-Chi and Gorkha. Locations with skyline angles of <20° have less than half the study area average landslide hazard for all inventories, while those with skyline angles of >50° have more than double the study area average (Figure 5a). The lowest landslide hazard values, at skyline angles of less than 10°, are lower than those for local slope or upslope contributing area. As with local slope, the curves for several of the inventories (Finisterre, Chi-Chi and Wenchuan) collapse to a similar relationship when normalised by study area average hazard, suggesting similar behaviour across a range of different landscapes. However, Northridge and Haiti show stronger sensitivity to skyline angle, and Gorkha shows considerably reduced landslide hazard at low skyline angles, relative to the other inventories. Some of this variability between inventories is likely related to differences in rock strength, because normalising skyline angle by the study area average considerably reduces the separation between individual curves, particularly those for Gorkha, Northridge and Haiti (Figure 5b).

Deleted: Page Break

Deleted: probability

Deleted:) as it does for

Deleted: probability

Deleted: probability

Deleted: of

Deleted: probability

Deleted: probability

Deleted: probability

Deleted: probability

Deleted: Northrige

Deleted: probability

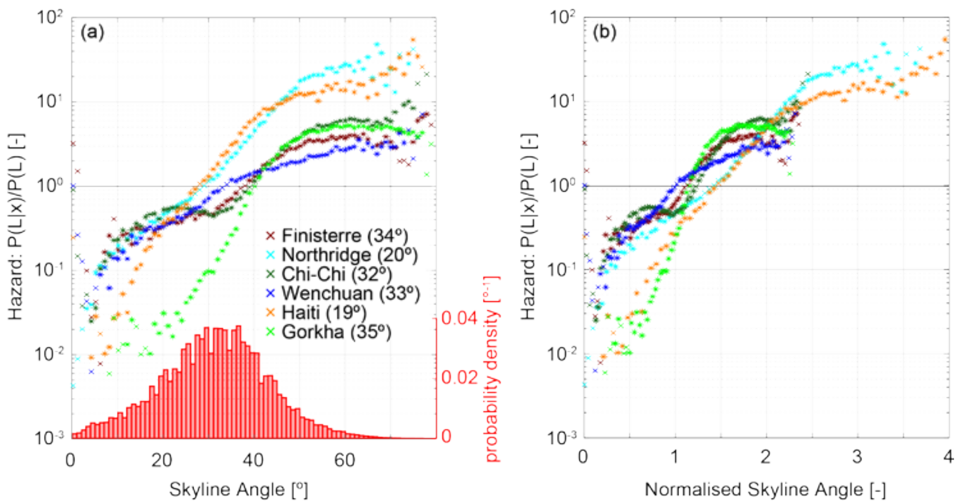

Figure 5. Landslide hazard defined as conditional landslide probability normalised by study area average landslide probability, for a) skyline angle; and b) skyline angle normalised by the study area average. Asterisks indicate values for which conditional probability differs from the study area average probability at 90% confidence. Red bars in (a) show histograms of skyline angle over the six inventories. Numbers in brackets show study area average skyline angles.

6.5. Hazard area

The ability of hazard area A_h to distinguish landslide from non-landslide cells is sensitive to two tuneable parameters (θ_m and θ_s in Equations 6 and 7), that have a unique optimum for each inventory (Figure S1). The optimum parameter values vary between inventories, with optimum initiation slopes θ_m ranging from 36˚ to 40˚ and stopping slopes θ_s from 6˚ to 31˚ (Table S1). Since these optimum parameters vary between inventories and can only be identified after an earthquake, they are problematic in terms of incorporation into a rule. Instead, we use the global averages of the optimised parameter values from the six inventories, θ_m = 40˚ and θ_s 10˚, rounded to one significant figure to simplify the rule (and because it involves changing only θ_m from 39˚ to 40˚). The stopping angle of 10˚ is steeper than many, though not all, of the observed slopes on which debris flows stop. For example, Stock and Dietrich (2003) reported that debris flows generally exhibit stopping angles of 2-6˚, but may halt at much larger angles (13-22˚) on open slopes. The steeper angles reported here

Deleted: highly

Deleted:) but follows a smooth optimisation surface with

Deleted: Optimum parameters

Deleted: average

Deleted: (θ

Deleted: 39˚

Deleted: report

Deleted: -flow

Deleted: ,

may reflect differences in the method and resolution of slope calculation but may result from the coseismic trigger, which does not necessitate high levels of saturation in the initial failure. Landslide hazard is very low for cells with A_h = 0 (i.e., where no cells steeper than the initiation angle runout over flowpaths steeper than the stopping angle), ranging from 2% to 15% of the study area average (Figure 6). Hazard increases with increasing A_h for all inventories but only slowly for A_h < 20 m^2/m; the trend then steepens to a peak (Northridge, Haiti, Nepal) or plateau (Finisterre, Chichi, Wenchuan) at A_h values of ~100 to 1000 m^2/m with conditional probabilities that are 200-800% of the study area average (Figure 6). For Finisterre and Wenchuan, a combination of limited observations and a weaker dependence of landslide probability on hazard area results in large parts of the curve (at A_h >1 m^2/m) where conditional probabilities cannot be distinguished from the study area average. For all sites, confidence becomes weak for hazard areas greater than 1000 m^2/m.

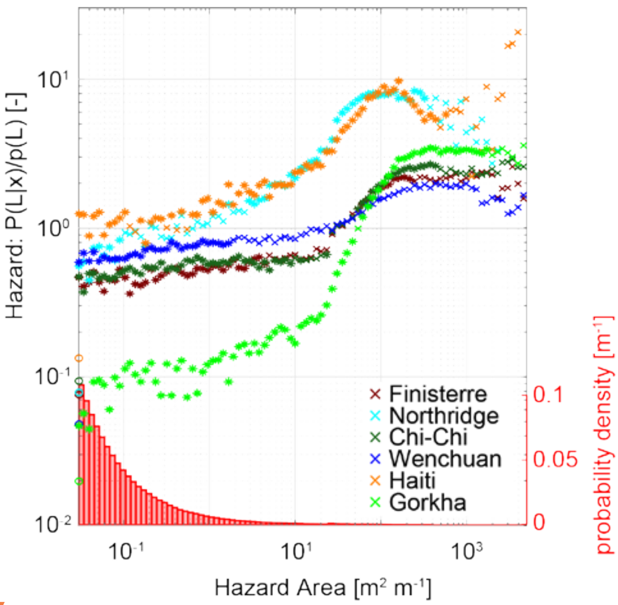

Figure 6. Landslide hazard defined as conditional landslide probability $P(L|x)$ normalised by study area average landslide probability $P(L)$, for hazard area. Hazard area is calculated with global average parameters θ_m and θ_s - that is, the areas with slope greater than 40° that have a flow path to the cell of interest and do not travel across a cell with a slope less than 10°. Coloured circles on the y-axis indicate landslide hazard for cells with a hazard area of 0 m^2/m. Asterisks indicate values

Deleted: likely

Deleted: Conditional probabilities are

Deleted: 5b). Conditional probability

Deleted: 1

Deleted: -

Deleted: 5b).

Deleted:

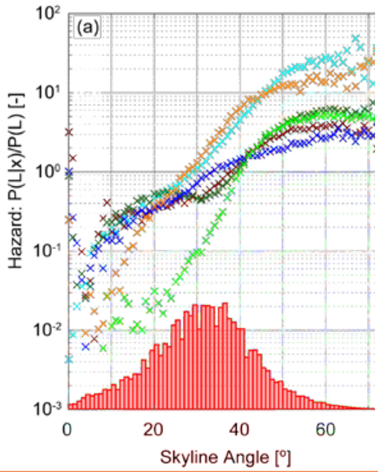

Deleted: 5

Formatted: Font: Italic

Formatted: Font: Italic

Deleted: a) skyline angle; and b)

Deleted: 39°

Deleted: Red bars show histograms of each variable over the six inventories.

Deleted: in (b)

Deleted: conditional probabilities

Deleted: Note logarithmic y-axes and different y-axis scales in panels a and b. The solid black lines show a normalised for which probability differs from the study area average at 90% confidence. Red bars show histograms of hazard area over the six inventories.

6.6. ROC analysis

To supplement conditional probability analysis, we examine the performance of slope, upslope contributing area, skyline angle, and hazard area as continuous hazard indices (with high index values reflecting high hazard and vice versa) using ROC curves (Figure 6). Successful hazard indices will capture landslide cells within high index zones (true positives) without capturing non-landslide cells in the same zones (false positives). Hazard area performs best for all six inventories with an AUC always above 0.78 and an average AUC of 0.83 (Table 1). Skyline angle performs joint best for Haiti and second best for a further three of the six inventories, with AUC always above 0.65 and an average AUC of 0.77. The exceptions, where slope, upslope area, or their combination perform second best, are Northridge and Wenchuan. For Northridge slope alone and slope plus upslope contributing area both outperform skyline angle by a single percentage point, while upslope contributing area by itself performs considerably worse (Figure 7a). For Wenchuan, upslope contributing area considerably outperforms the other indices, while slope performs particularly poorly, perhaps reflecting longer-runout landslides that extend to lower slopes and larger areas (Figure 7d). Although slope, upslope contributing area, and their combination all perform better than skyline angle in one of the inventories, none of these metrics do so consistently across multiple inventories. This is reflected in their averaged AUC values over all inventories of 0.69, 0.72 and 0.74 for upslope contributing area, slope, and their combination respectively.

Table 1. Area under the ROC curve for the five hazard metrics over the six coseismic landslide inventories. The best performing metric for each inventory is in bold, the second best is in italics and the worst performing metric is underlined.

	Hazard area	Skyline angle	Slope + upslope contributing area	Local slope	Upslope contributing area
Finisterre	**0.79**	*0.72*	0.69	0.69	0.66
Northridge	**0.89**	0.83	*0.84*	*0.84*	0.62

Deleted: of 1, equivalent to
Deleted: ; thus, points above the solid black line have conditional probability greater than the study
Deleted: average
Deleted: hazard
Deleted: performs
Deleted:
Deleted: 6a
Deleted: in this inventory, while slope performs particularly poorly
Deleted: 6d
Deleted: .
Deleted: 72
Deleted: 73
Deleted: slope,
Formatted: Underline
Formatted: Underline

Chi-Chi	**0.80**	*0.73*	0.68	0.67	0.69
Wenchuan	**0.78**	0.65	0.62	0.58	*0.74*
Haiti	**0.86**	*0.85*	0.83	0.79	0.69
Gorkha	**0.88**	*0.85*	0.77	0.73	0.76
Average	0.83	0.77	0.74	0.72	0.69
1σ	0.05	0.08	0.09	0.09	0.05

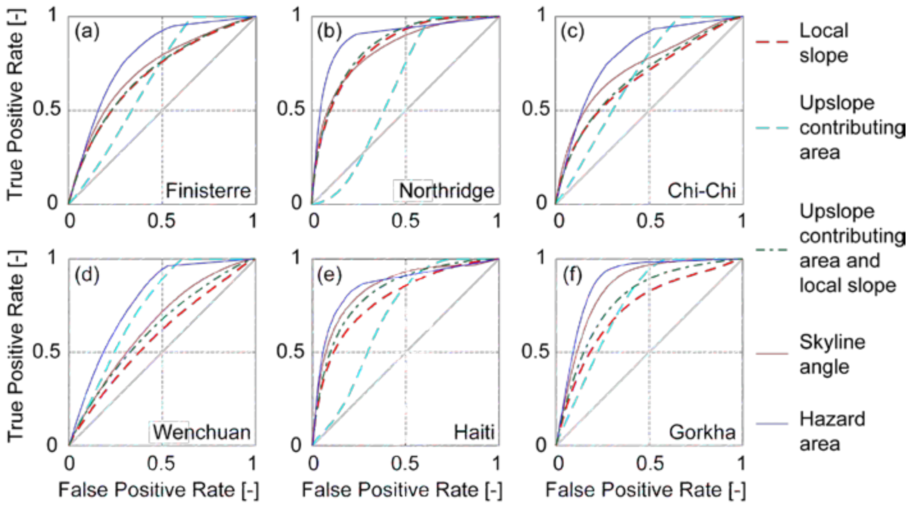

Figure 7. Receiver operating characteristic (ROC) curves for the six inventories: a) Finisterre, b) Northridge, c) Chi-Chi, d) Wenchuan, e) Haiti, f) Gorkha. False positive rate is given by the number of false positives divided by the sum of false positives and true negatives. True positive rate is given by the number of true positives divided by the sum of true positives and false negatives. The 1:1 line represents the naïve random case. Curves plotting closer to the top left corner of each panel represent better model performance.

7. Discussion

We structure the discussion around three simple rules that are drawn from the results above. In each case we explain the evidence on which the message is based, why it works, our degree of confidence, and implications for applying the rule. Finally, we examine the spatial implications of these rules using an example landscape.

Formatted: Underline

Formatted: Underline

Formatted: Underline

Formatted: Underline

Deleted: Page Break ¶

Deleted: 6

Deleted: (

Deleted:)

7.1. Rule 1: Avoid steep (>10˚) channels with many steep (>40˚) areas that are upslope

The hazard area is the best or joint-best predictor of landslide hazard for all six inventories. The hazard area defined by the average initiation angle (40°) and stopping angle (10°) across all six inventories performs nearly as well as the optimised area for each inventory, enabling us to define a general rule independent of any specific inventory. This is fortunate, as site-specific optimisation requires a pre-existing landslide inventory for any individual area and so may not be generally feasible. In all six inventories, locations with A_h > 60 m^2/m have landslide hazard that is greater than the study area average. While landslide hazard generally increases with increasing hazard area, the relationship is complex (Figure 6). Landslide hazard can be most effectively decreased by decreasing A_h in the range 20-100 m^2/m. Outside of this range A_h is less related to hazard. An exception to this pattern is seen in areas with a hazard area of zero, which generally have landslide hazard 5-10 times lower than that for even for very small values of A_h (c. 0.1 m^2/m). On this basis, the qualitative statement to avoid areas with 'many' steep slopes could also be phrased as 'any' steep slopes.

7.2. Rule 2: Minimise your maximum angle to the skyline

The maximum skyline angle is the second-best predictor of landslide hazard in four of the six cases. Locations with skyline angles less than 30˚ generally have a landslide hazard below the study area average. Importantly, landslide hazard increases non-linearly with skyline angle, so that a slight reduction to a high skyline angle results in a much larger reduction in hazard than a similar reduction to a lower skyline angle.

The distinction between local slope and skyline angle reflects the importance of runout as well as initiation in defining landslide hazard. Landslide hazard is an inherently non-local problem, defined by both conditions at the point of interest and those upslope of that point. The skyline angle is a simple way to represent this. It has the additional advantage of being easy to measure, needing only a protractor or clinometer for precise measurement in the field, and being easily approximated by eye. Local slope (rule 3), in contrast, is scale-dependent, while hazard area A_h (rule 1) is considerably more difficult to estimate in the field.

Deleted: avoid

Deleted: 39˚

Deleted:

Deleted: probability

Deleted: 39

Deleted: probability above

Deleted: probability

Deleted: at intermediate values

Deleted: , whereas decreasing A_h at either the upper or lower extremes has minimal effect on

Deleted: The

Deleted: since the landslide probability is generally 5-10 times higher even for very small values of A_h (c. 0.1 m^2/m) than the landslide probability for areas with no A_h.

Deleted: Landslides do not always obey steepest

Moved down [3]: flow path routing rules, and it is possible for landslides to travel up reverse slopes or along contours. This is particularly true for large deep-seated landslides or rockfalls. The hazard area metric cannot account for such behaviour and thus is more likely to reflect hazard from smaller shallow landslides, while skyline angle, which does allow for runout over reverse slopes, may be a better predictor for larger deep-seated landslides. The two indices have some overlap but could be used in combination to find safer locations in the landscape.¶
¶

Formatted: Font: +Body (Calibri)

Deleted: probability

Deleted: probability

Deleted: probability

Deleted: landslide probability

Deleted: it would for

Deleted: ,

Deleted: upslope contributing

Deleted: and

Deleted: are both

Landslides do not always obey flow path routing rules, and it is possible for landslides to travel up reverse slopes or along contours. This is particularly true for large deep-seated landslides or rockfalls. The hazard area metric cannot account for such behaviour and thus is more likely to reflect hazard from smaller shallow landslides, while skyline angle, which does allow for runout over reverse slopes, may be a better predictor for larger deep-seated landslides. The two indices have some overlap but could be used in combination to find safer locations in the landscape.

7.3. Rule 3: Minimise the angle of the slope under your feet, especially on steep hillsides, but not at the expense of increasing skyline angle or hazard area

Local slope generally performs less well than skyline angle or hazard area, but is still a consistently skilful predictor of coseismic landslide hazard, and could be a useful additional discriminant for situations where both skyline angle and hazard area are comparable between two locations. In this situation, our results suggest choosing the location with the lower local slope. This is particularly true at steeper slopes since landslide hazard increases exponentially with slope, approximately doubling for every 10˚ increase in slope.

Given the observation from a number of landslide inventories that coseismic landslides initiate near ridge crests (Densmore and Hovius, 2000; Meunier et al., 2008; Rault et al., 2018), it is perhaps surprising that landslide hazard generally increases with increasing upslope contributing area (i.e., when moving downslope from ridge crests). In fact, while coseismic landslides may initiate preferentially near the ridges, they run out downslope; thus, areas near ridges are less likely to be touched by any part of a landslide even though they are more likely than other parts of the landscape to contain the top of a landslide scar. Landslide hazard is consistently low at small values of upslope contributing area, corresponding to ridges; for some inventories, it is also low at very large values of upslope contributing area, corresponding to valley floors in the downstream reaches of the river network. This may be partly a function of the covariance between local slope and upslope contributing area, because locations with large upslope contributing areas generally have lower slopes (see dashed lines in Figure 4). The addition of upslope contributing area as a predictor in logistic regression improves landslide hazard prediction relative to slope alone (Table 1), but the orientation of the logistic regression contours (Figure 4) indicates that its influence is weak. Moving

Moved (insertion) [3]

Formatted: Font: +Body (Calibri)

Formatted: Left, Space After: 10 pt, Line spacing: Multiple 1.15 li

Deleted: ¶

Deleted: local

Deleted: slopes, and even at the expense of increasing upslope contributing area

Deleted: probability

Deleted: common

Deleted: 2007

Deleted: .

Deleted: runout

Deleted: crest

Deleted: probability

Deleted: very low

Deleted: high

Deleted: since

Deleted: probability

Deleted: probability

to a location with lower slope angle almost always reduces landslide hazard independently of the upslope contributing area of the new location, although the specific reduction of landslide probability depends on the shape of the two-dimensional probability surface (Figure 4). These results suggest that decisions on how to reduce landslide hazard most effectively need to be made on a case by case basis, and are best made using hazard area, skyline angle, and the local slope in conjunction with each other. Steep areas that are upslope of a given location result in elevated hazard but gentle areas do not, explaining the improved performance of hazard area relative to upslope contributing area (Figure 6 and Table 1). Ridges, with very low upslope contributing area, are generally low hazard locations if they have gentle local slope, but can still be hazardous if they are steep (Figure 4). To minimise landslide hazard, it is thus preferable to seek broad ridges over sharp ridges where such a choice is possible.

7.4. Movement rules in a landscape with variable hazard

Our analysis is focused on cell-by-cell hazard assessment, and is thus most appropriate for decision-making before the next large earthquake. However, it is also possible to use our results to inform movement or relocation during or immediately after an earthquake, when it is likely that movement will be limited to small distances. Our analysis shows that, even during a large earthquake in mountainous terrain, landslide hazard is not ubiquitously high. A significant fraction of the landscape has low landslide hazard (<5% of the study area average) – as much as 30% in Northridge and 33% in Nepal. Landslide hazard is extremely granular in spatial terms, so that small changes in location can make a big difference to exposure. This means that it is often possible to find nearby locations with lower landslide hazard, irrespective of the starting point. The vast majority of locations (75% in Nepal, 95% in Northridge) are within 1 km of areas of low landslide hazard (<5% of the study area average). Even smaller movements of 100 m or less, as might be possible during or immediately after a large earthquake, can result in very large reductions in hazard.

Detailed analysis in the Northridge (Figure 8) and Nepal inventories shows that landslide hazard can often be effectively reduced by moving: from a slope to a ridge (e.g., from A to B in Figure 8, a 190% reduction in landslide hazard); out of a gully (e.g., from C to D, a 100% reduction), or downstream of a flatter area (e.g., from C to E a 100% reduction). However, there is no single answer to the question

Deleted: probability

Deleted: We conclude

Deleted: areas

Deleted: upslope

Deleted: While this

Deleted: a

Deleted: the

Deleted: define some rules for

Deleted: .

Deleted: probability

Deleted: This means that it is often possible to find locations with lower landslide hazard.

Deleted: probability

Deleted: 7

Deleted: 7),

of where to move to reduce coseismic landslide hazard, since this differs depending on the setting, the distance that can be travelled due to time or location constraints, and on the chosen rule (e.g., skyline angle vs. hazard area). Given a 1 km radius of potential movement, minimizing skyline angle involves moving upslope for ~75% of locations in Nepal but only ~66% in Northridge. In some cases, knowing how far one can travel can be critical: if one may only travel a short distance, moving upslope may be preferable (e.g., from C to D in Figure 8, a 100% reduction), while if one could travel farther, moving downslope may offer greater hazard reduction (e.g., from C to F or G, a 120% or 190% reduction respectively).

Deleted: 7

Landslide hazard estimates for high hazard locations are broadly comparable between skyline angle and hazard area metrics (e.g. Figure 8). However, different metrics emphasise different parts of the landscape. Ridges consistently minimise skyline angle but may still have intermediate values of hazard area if the ridge is sharp so that the local slope of the ridge itself is steep. Broad valley floors consistently minimise hazard area, but may still have intermediate values of skyline angle if the neighbouring slopes have sufficient relief. There are trade-offs between these metrics, and further work is needed into how they might be combined to further reduce hazard.

Deleted: probability

Deleted: 7

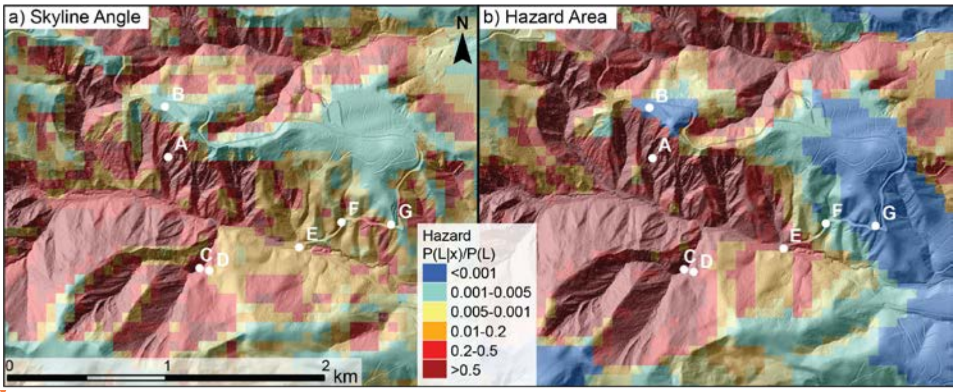

Deleted:

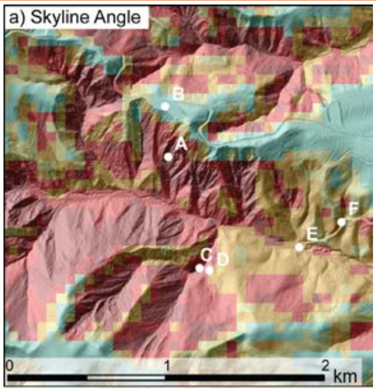

Figure 8. Example landslide hazard estimates derived from a) skyline angle and b) hazard area for a small section of the Northridge study area. Colours reflect landslide hazard estimated from the two methods, expressed as a fraction of the study area average hazard. Points labelled A-G in white are example locations discussed in Section 7.4. Hazard estimates are overlain on a shaded

Deleted: 7

Deleted:

relief image derived from a 0.5 m resolution LiDAR DEM for context (source: NCALM, 2015, DOI:10.5069/G9TB14V2).

7.5 Caveats

These rules should be combined with existing guidance, such as local knowledge and formal hazard and risk information when that is available. The rules provide an evidence base that could be used, for example, in infrastructure and land-use planning, identifying evacuation routes, and designing contingency plans from individual to community level, where more detailed or formal technical advice is not available. It is also important to note some caveats.

This analysis is purely focussed on coseismic landslide hazard, and thus it does not take into account the distribution of vulnerability: that is, the locations of people and infrastructure in these landscapes or how they might be differentially impacted by landslides. While one area may be more hazardous than another, the distribution of people and infrastructure may be such that risk is not actually increased. Further, our analysis is probabilistic, defining hazard as the probability of intersecting a landslide; thus, our rules identify locations where the landslide probability is lower, not where probability is zero. This means that it is possible for an alternate location chosen based on its lower landslide probability to be impacted by a landslide while the original higher-probability location is not. The choice of inventory will influence the specific results and, although we adjust for bulk shaking intensity by normalising conditional probability by bulk probability, differences between inventories are likely to remain (e.g., in spatial patterns of shaking intensity and their relation to topography). Rock type is a critical influence on landslide occurrence (Chen et al., 2012; Harp et al., 2016; Roback et al., 2018), but we have excluded it from our analysis because it is extremely difficult for an untrained observer to identify and to translate into meaningful estimates of material strength and thus landslide probability. We also expect that the length scales over which lithology varies will often be long (on the order of kilometres) relative to the other factors examined here.

Because the analysis is focussed on coseismic landslide hazard, it does not account for other sources of hazard, either associated with an earthquake (e.g., amplification of seismic accelerations on ridges), or with other processes or events such as flooding or rainfall-induced landsliding. In some cases, following our rules in isolation might increase exposure to other hazards. For example,

Formatted: Font: Not Italic

Deleted: While rock type is likely to influence the relationship between topography and landslide hazard (e.g., Chen et al., 2012) we

Deleted: this occurs to

Formatted: Font: Not Italic

Deleted: seismic

Formatted: English (United States)

moving to ridge tops to minimise skyline angle might increase exposure to intense shaking due to seismic amplification in subsequent earthquakes; moving to valley floors that are occupied by large rivers, where hazard area is minimal, might increase exposure to fluvial flooding. We have also not considered the effects of landslide size or failure type, choosing instead to treat all landslides as representing an equivalent hazard. If landslide size or type shows a strong spatial dependence, then parts of the landscape may be preferentially impacted in ways that are not reflected by our rules. It is not yet clear how transferrable our conditional probability results are to rainfall-triggered landslides. For instance, stopping angles are likely to be lower for rainfall-triggered landslides if the failing mass is more highly saturated (e.g., Stock and Dietrich, 2003), meaning that the hazard area in rule 1 underestimates potential landslide impacts. Similarly, in the case of rainfall-triggered landslides, initiation is likely to depend not only on slope angle but also on a topographic control on saturation (e.g. Montgomery and Dietrich, 1994). Extending the analysis to other triggering mechanisms is thus a future research need.

We have evaluated these rules using gridded topographic data and landslide inventories. Topographic derivatives, particularly slope and upslope contributing area, are known to be sensitive to the resolution of the DEM from which they are derived. We use the Northridge study site to begin to explore this issue, by repeating our analysis with DEMs at both the original 10 m resolution and at resampled resolutions of 20, 30, 60, and 90 m. We find that performance of slope, skyline angle, and upslope contributing area all improve slightly at finer resolutions (Table S3). Hazard area performance degrades at both finer and coarser resolutions than 30 m, likely the result of parameter optimization being performed at 30m resolution. We still find, however, that the hazard area metric remains the most skillful predictor of landslide hazard across all DEM resolutions.

The accuracy of landslide inventories depends on the quality of the imagery from which they are mapped and on subjective judgements by the mappers (Williams et al., 2018). For example, there are uncertainties associated with landslide distinction and amalgamation (Marc et al., 2015; Tanyas et al., 2017), and the definition of the downslope boundary of each landslide. Amalgamation is particularly problematic for landslide volume estimates but less so in our analysis, which requires identification of landslide affected areas rather than distinguishing individual landslides. However, recent studies have identified substantial areal mismatches (up to 67%) between inventories of the

Deleted: have

Deleted: Finally, it

Deleted: where

Deleted: .

Deleted:).

Deleted: Bellugi et al., 2011

same event mapped by different authors (Fan et al., 2019). To investigate the impact of mapping error on our results, we test two independent inventories for the Wenchuan earthquake, from Li et al. (2014) and Xu et al. (2014b), with an estimated areal mismatch for our study area of 21%. We find that the change of inventory has no impact on the rank order of performance of the metrics (Table S3); and a minor impact on both the AUC values and the hazard curves (Figures S10 and S11). Thus, we suggest that our findings are relatively robust to mapping uncertainties in the landslide inventories that we have used.

8. Conclusions

We have defined a set of simple rules that can be used to anticipate, and thus potentially reduce, exposure to earthquake-triggered landslides. We test a set of candidate predictors for their ability to reproduce mapped landslide distributions from six recent earthquakes. Landslide hazard, defined as the conditional probability of intersecting a landslide in one of the six earthquakes, increases exponentially with local slope. Landslide hazard on hillslopes also increases with upslope contributing area, suggesting that while ridges may be areas of preferential coseismic landslide initiation, they are not the locations of highest coseismic landslide hazard due to downslope movement of landslide material during runout. When accounting for both slope and upslope contributing area, landslide hazard is highest for the largest upslope contributing area at a given slope or the highest slope at a given upslope contributing area. Landslide hazard can be reduced by decreasing local slope, even at the cost of increased upslope contributing area, and especially at high slopes. Landslide hazard also increases exponentially with the skyline angle, and this simple, easily-measured metric performs better than slope or upslope contributing area for four of the six inventories. Hazard area, which accounts for both landslide initiation and runout, offers the best predictive skill for all six inventories but is more difficult to estimate in the field and requires estimation of two empirical parameters. Fortunately, hazard area calculated with parameters that are averaged across all six study sites (initiation angle of 40° and stopping angle of 10°) performs almost as well as hazard area calculated with optimised site-specific parameters, suggesting that the average parameters can be applied to other inventories. These findings can be distilled into three simple rules:

Deleted: introduced
Deleted: identify
Deleted: highest
Deleted: reducing
Deleted: ,
Deleted: 39°
Deleted: only slightly worse than

1) Avoid steep (>10˚) channels with many steep (>40˚) areas that are upslope;
2) Minimise your maximum angle to the skyline; and
3) Minimise the angle of the slope under your feet, especially on steep hillsides, but not at the expense of increasing skyline angle or hazard area.

Acknowledgements

This work was financially supported by grants from the NERC/ESRC Increasing Resilience to Natural Hazards programme (NE/J01995X/1) and the NERC/ESRC/NNSFC Increasing Resilience to Natural Hazards in China programme (NE/N012216/1). We thank: 1) colleagues at the National Society for Earthquake Technology-Nepal (NSET) who have helped to shape our thinking on landslide hazard and the challenge of risk communication; 2) those responsible for collecting the landslide inventories used in this study, particularly Niels Hovius and contributors to the ScienceBase-Catalog; and 3) William Dietrich and Niels Hovius for helpful comments on an earlier draft. Gianvito Scaringi, Odin Marc, and an anonymous reviewer provided constructive and illuminating comments and suggestions that considerably refined our thinking. LiDAR data acquisition and processing were completed by the National Center for Airborne Laser Mapping (NCALM). NCALM funding was provided by NSF's Division of Earth Sciences, Instrumentation and Facilities Program (EAR-1043051). MATLAB code for the computation of skyline angles is available at: https://github.com/DavidMilledge.

References

Alexander, D.: Vulnerability to landslides. In *Landslide Hazard and Risk. Wiley, Chichester*, pp.175-198. 2005.

Atwater B.F., Cisternas M.V., Bourgeois J., Dudley W.C., Hendley J.W., and Stauffer P.H.: Surviving a tsunami--lessons from Chile, Hawaii, and Japan (No. 1187). Geological Survey (USGS). 1999.

Deleted: 39˚

Deleted: local

Deleted: slopes and even at the expense of increasing upslope contributing area

Deleted: Neils

Deleted: those that contributed their data

Deleted: Neils

Deleted: .

Formatted: Indent: First line: 0.5 cm

Deleted: Abbott, L.D., Silver, E.A., Anderson, R.S., Smith, R., Ingle, J.C., Kling, S.A., Haig, D., Small, E., Galewsky, J. and Sliter, W.S.: Measurement of tectonic surface uplift rate in a young collisional mountain belt. *Nature*, *385*(6616), pp.501-507. 1997.¶

Avouac, J.P., Meng, L., Wei, S., Wang, T. and Ampuero, J.P.: Lower edge of locked Main Himalayan Thrust unzipped by the 2015 Gorkha earthquake. *Nature Geoscience*, *8*(9), p.708. 2015.

Bellugi, D., Dietrich, W.E., Stock, J., McKean, J., Kazian, B. and Hargrove, P.: Spatially explicit shallow landslide susceptibility mapping over large areas. *Proceedings of the 5th International Conference on Debris-Flow Hazards Mitigation: Mechanics, Prediction and Assessment, Italian Journal of Engineering Geology and Environment. 759-768*. DOI: 10.4408/IJEGE.2011-03.B-045. 2011.

Benda, L.E. and Cundy, T.W.: Predicting deposition of debris flows in mountain channels. *Canadian Geotechnical Journal*, *27*(4), pp.409-417. 1990.

Berti, M., Martina, M. L. V., Franceschini, S., Pignone, S., Simoni, A., & Pizziolo, M. Probabilistic rainfall thresholds for landslide occurrence using a Bayesian approach. *Journal of Geophysical Research: Earth Surface*, 117, F04006. 2012.

Blöthe, J.H., Korup, O. and Schwanghart, W.: Large landslides lie low: Excess topography in the Himalaya-Karakoram ranges. *Geology*, *43*(6), pp.523-526. 2015.

Briggs, J.: The use of indigenous knowledge in development: problems and challenges. *Progress in Development Studies*, 5(2): 99-114. 2005.

Chen, X.L., Ran, H.L. and Yang, W.T.: Evaluation of factors controlling large earthquake-induced landslides by the Wenchuan earthquake. *Natural Hazards and Earth System Sciences*, *12*(12), pp.3645-3657. 2012.

Claessens, L., Heuvelink, G.B.M., Schoorl, J.M. and Veldkamp, A.: DEM resolution effects on shallow landslide hazard and soil redistribution modelling. *Earth Surface Processes and Landforms*, *30*(4), pp.461-477. 2005.

Corominas, J.: The angle of reach as a mobility index for small and large landslides. *Canadian Geotechnical Journal*, *33*(2), pp.260-271. 1996.

Dadson, S.J., Hovius, N., Chen, H., Dade, W.B., Hsieh, M.L., Willett, S.D., Hu, J.C., Horng, M.J., Chen, M.C., Stark, C.P. and Lague, D.: Links between erosion, runoff variability and seismicity in the Taiwan orogen. *Nature*, *426*(6967), pp.648-651. 2003.

Formatted: Indent: First line: 0.5 cm

Deleted:

Formatted: Indent: First line: 0.5 cm

Deleted: Bookhagen, B. and Burbank, D.W.: Topography, relief, and TRMM-derived rainfall variations along the Himalaya. *Geophysical Research Letters*, *33*(8). 2006.¶

Deleted: Burchfiel, B.C., Zhiliang, C., Yupinc, L. and Royden, L.H.: Tectonics of the Longmen Shan and adjacent regions, central China. *International Geology Review*, *37*(8), pp.661-735. 1995.¶

Deleted: Chi, W.C., Dreger, D. and Kaverina, A.: Finite-source modeling of the 1999 Taiwan (Chi-Chi) earthquake derived from a dense strong-motion network. *Bulletin of the Seismological Society of America*, *91*(5), pp.1144-1157. 2001.¶
Churches, C.E., Wampler, P.J., Sun, W. and Smith, A.J.: Evaluation of forest cover estimates for Haiti using supervised classification of Landsat data. *International Journal of Applied Earth Observation and Geoinformation*, *30*, pp.203-216. 2014.¶

Deleted: Colburn, I.P., Saul, L.E.R. and Almgren, A.A.: The Chatsworth Formation: a new formation name for the Upper Cretaceous strata of the Simi Hills, California. 1981.¶
Craddock, W.H., Burbank, D.W., Bookhagen, B. and Gabet, E.J.: Bedrock channel geometry along an orographic rainfall gradient in the upper Marsyandi River valley in central Nepal. *Journal of Geophysical Research: Earth Surface*, *112*(F3). 2007.¶

Dai, F.C., Xu, C., Yao, X., Xu, L., Tu, X.B. and Gong, Q.M.: Spatial distribution of landslides triggered by the 2008 Ms 8.0 Wenchuan earthquake, China. *Journal of Asian Earth Sciences*, *40*(4), pp.883-895. 2011.

Datta, A., Sigdel, S., Oven, K., Rosser, N., Densmore, A., Rijal, S.: The role of scientific evidence during the 2015 Nepal earthquake relief efforts. *Overseas Development Institute: London, UK*.: 2018.

Densmore, A.L., Ellis, M.A. and Anderson, R.S.: Landsliding and the evolution of normal-fault-bounded mountains. *Journal of geophysical research: solid earth*, *103*(B7), pp.15203-15219. 1998.

Densmore, A.L. and Hovius, N.: Topographic fingerprints of bedrock landslides. *Geology*, *28*(4), pp.371-374. 2000.

Dietrich, W.E. and Sitar, N.: Geoscience and geotechnical engineering aspects of debris-flow hazard assessment. In *Debris-flow hazards mitigation: Mechanics, prediction, and assessment* (pp. 656-676). ASCE. 1997.

Dransch, D., Rotzoll, H. and Poser, K.: The contribution of maps to the challenges of risk communication to the public. *International Journal of Digital Earth*, *3*(3), pp.292-311. 2010.

Fan, X., Scaringi, G., Domènech, G., Yang, F., Guo, X., Dai, L., He, C., Xu, Q. and Huang, R.: Two multi-temporal datasets that track the enhanced landsliding after the 2008 Wenchuan earthquake. *Earth System Science Data*, *11*(1), pp.35-55. 2019.

Fannin, R.J. and Wise, M.P.: An empirical-statistical model for debris flow travel distance. *Canadian Geotechnical Journal*, *38*(5), pp.982-994. 2001.

Fell, R., Ho, K.K., Lacasse, S. and Leroi, E.: A framework for landslide risk assessment and management. *Landslide risk management*, pp.3-25. 2005.

Froude, M.J., and Petley, D.: Global fatal landslide occurrence from 2004 to 2016. *Natural Hazards and Earth System Sciences*, 18, pp.2161-2181. 2018.

George, D.L. and Iverson, R.M.: A depth-averaged debris-flow model that includes the effects of evolving dilatancy: 2. Numerical predictions and experimental tests *Proc. R. Soc. Lond. Ser. A*, 470 p. 20130820. 2014.

Frattini, P., Crosta, G. and Carrara, A.: Techniques for evaluating the performance of landslide susceptibility models. *Engineering geology*, *111*(1-4), pp.62-72. 2010.

Deleted: Davies, H.L., Lock, J., Tiffin, D.L., Honza, E., Okuda, Y., Murakami, F. and Kisimoto, K.: Convergent tectonics in the Huon Peninsula region, Papua New Guinea. *Geo-Marine Letters*, *7*(3), pp.143-152. 1987.¶

Moved down [4]: Densmore, A.L.,

Deleted: Ellis, M.A., Li, Y., Zhou, R., Hancock, G.S. and Richardson, N.: Active tectonics of the Beichuan and Pengguan faults at the eastern margin of the Tibetan Plateau. *Tectonics*, *26*(4). 2007.¶

Formatted: English (United States)

Deleted: Elliott, J.R., Jolivet, R., González, P.J., Avouac, J.P., Hollingsworth, J., Searle, M.P. and Stevens, V.L.: Himalayan megathrust geometry and relation to topography revealed by the Gorkha earthquake. *Nature Geoscience*, *9*(2), pp.174-180. 2016.¶
Escuder-Viruete, J., Pérez-Estaún, A., Contreras, F., Joubert, M., Weis, D., Ullrich, T.D. and Spadea, P.: Plume mantle source heterogeneity through time: Insights from the Duarte Complex, Hispaniola, northeastern Caribbean. *Journal of Geophysical Research: Solid Earth*, *112*(B4). 2007.¶

Formatted: Indent: First line: 0.5 cm

Formatted: Indent: First line: 0.5 cm

Geller, R.J.: Earthquake prediction: a critical review. *Geophysical Journal International*, *131*(3), pp.425-450. 1997.

Gigerenzer, G.: Why heuristics work. *Perspectives on psychological science*, *3*(1), pp.20-29. 2008.

Gorum, T., Fan, X., van Westen, C.J., Huang, R.Q., Xu, Q., Tang, C. and Wang, G.: Distribution pattern of earthquake-induced landslides triggered by the 12 May 2008 Wenchuan earthquake. *Geomorphology*, *133*(3), pp.152-167. 2011.

Gorum, T., Korup, O., van Westen, C.J., van der Meijde, M., Xu, C. and van der Meer, F.D.: Why so few? Landslides triggered by the 2002 Denali earthquake, Alaska. *Quaternary Science Reviews*, *95*, pp.80-94. 2014.

Guillard-Gonçalves, C., Zêzere, J.L., Pereira, S. and Garcia, R.A.C.: Assessment of physical vulnerability of buildings and analysis of landslide risk at the municipal scale: application to the Loures municipality, Portugal. *Natural Hazards & Earth System Sciences*, *16*(2). 2016.

Hancock, G.R. and Evans, K.G.: Channel head location and characteristics using digital elevation models. *Earth Surface Processes and Landforms*, *31*(7), pp.809-824. 2006.

Harp, E.L., Wilson, R.C. and Wieczorek, G.F.: *Landslides from the February 4, 1976, Guatemala earthquake*(No. 551.3 HAR). US Government Printing Office. 1981.

Harp, E.L. and Jibson, R.W.: Landslides triggered by the 1994 Northridge, California, earthquake. *Bulletin of the Seismological Society of America*, *86*(1B), pp.S319-S332. 1996.

Harp, E.L., Jibson, R.W., and Schmitt, R.G.: Map of landslides triggered by the January 12, 2010, Haiti earthquake: U.S. Geological Survey Scientific Investigations Map 3353, 15 p., 1 sheet, scale 1:150,000, http://dx.doi.org/10.3133/sim3353. 2016.

Harp, E.L., Jibson, R.W., Schmitt, R.G.: Map of landslides triggered by the January 12, 2010, Haiti earthquake, https://doi.org/10.5066/F7C827SR, in Schmitt, R.G., Tanyas, Hakan, Nowicki Jessee, M.A., Zhu, J., Biegel, K.M., Allstadt, K.E., Jibson, R.W., Thompson, E.M., van Westen, C.J., Sato, H.P., Wald, D.J., Godt, J.W., Gorum, Tolga, Xu, Chong, Rathje, E.M., Knudsen, K.L., 2017, An Open Repository of Earthquake-triggered Ground Failure Inventories, U.S. Geological Survey data release collection, accessed July 18, 2018, at https://doi.org/10.5066/F7H70DB4. 2017.

Deleted: Godard, V., Lavé, J., Carcaillet, J., Cattin, R., Bourlès, D. and Zhu, J.: Spatial distribution of denudation in Eastern Tibet and regressive erosion of plateau margins. *Tectonophysics*, *491*(1), pp.253-274. 2010.¶
Godard, V., Bourlès, D.L., Spinabella, F., Burbank, D.W., Bookhagen, B., Fisher, G.B., Moulin, A. and Léanni, L.: Dominance of tectonics over climate in Himalayan denudation. *Geology*, *42*(3), pp.243-246. 2014.¶

Deleted: van Westen, C.J., Korup, O., van der Meijde, M., Fan, X. and van der Meer, F.D.: Complex rupture mechanism and topography control symmetry of mass-wasting pattern, 2010 Haiti earthquake. *Geomorphology*, *184*, pp.127-138. 2013.¶
Gorum, T.,

Deleted: Griffith, G.E., Omernik, J.M., Smith, D.W., Cook, T.D., Tallyn, E., Moseley, K., and Johnson, C.B.: Ecoregions of California (poster): U.S. Geological Survey Open-File Report 2016–1021, with map, scale 1:1,100,000, http://dx.doi.org/10.3133/ofr20161021. 2016.¶

Hauksson, E., Jones, L.M. and Hutton, K.: The 1994 Northridge earthquake sequence in California: Seismological and tectonic aspects. *Journal of Geophysical Research: Solid Earth*, *100*(B7), pp.12335-12355. 1995.

Hayes, G.P., Briggs, R.W., Sladen, A., Fielding, E.J., Prentice, C., Hudnut, K., Mann, P., Taylor, F.W., Crone, A.J., Gold, R. and Ito, T.: Complex rupture during the 12 January 2010 Haiti earthquake. *Nature Geoscience*, *3*(11), p.800. 2010.

Hayes, G.P., Briggs, R.W., Barnhart, W.D., Yeck, W.L., McNamara, D.E., Wald, D.J., Nealy, J.L., Benz, H.M., Gold, R.D., Jaiswal, K.S. and Marano, K.: Rapid characterization of the 2015 M w 7.8 Gorkha, Nepal, earthquake sequence and its seismotectonic context. *Seismological Research Letters*, *86*(6), pp.1557-1567. 2015.

Heim, A.: *Bergsturz und menschenleben* (No. 20). Fretz & Wasmuth. 1932.

Huang, R. and Fan, X.: The landslide story. *Nature Geoscience*, *6*(5), pp.325-326. 2013.

Hunter, G. and Fell, R.: Travel distance angle for" rapid" landslides in constructed and natural soil slopes. *Canadian Geotechnical Journal*, *40*(6), pp.1123-1141. 2003.

Jaboyedoff, M., Baillifard, F., Couture, R., Locat, J. and Locat, P.: Toward preliminary hazard assessment using DEM topographic analysis and simple mechanical modeling by means of sloping local base level. *Landslides: evaluation and stabilization. Balkema, Taylor & Francis Group, London*, pp.199-206. 2004.

Keefer, D.K.: Statistical analysis of an earthquake-induced landslide distribution—the 1989 Loma Prieta, California event. *Engineering geology*, *58*(3), pp.231-249. 2000.Kennedy, I.T., Petley, D.N., Williams, R. and Murray, V.: A systematic review of the health impacts of mass Earth movements (landslides). *PLoS currents*, 7. 2015.

Kahneman, D. and Klein, G.: Conditions for intuitive expertise: a failure to disagree. *American Psychologist*, *64*(6), p.515. 2009.

Khazai, B., Sitar, N.: Evaluation of factors controlling earthquake-induced landslides caused by Chi-Chi earthquake and comparison with the Northridge and Loma Prieta events. *Engineering Geology*. 2004. https://doi.org/10.1016/S0013-7952(03)00127-3 .

Formatted: Indent: First line: 0.5 cm

Deleted: Hodges, K.V., Parrish, R.R. and Searle, M.P. Tectonic evolution of the central Annapurna range, Nepalese Himalayas. *Tectonics*, *15*(6), pp.1264-1291. 1996.¶
Hovius, N., Stark, C.P., Tutton, M.A. and Abbott, L.D.: Landslide-driven drainage network evolution in a pre-steady-state mountain belt: Finisterre Mountains, Papua New Guinea. *Geology*, *26*(12), pp.1071-1074. 1998.¶

Deleted: ¶
Libohova, Z., Wysocki, D., Schoeneberger, P., Reinsch, T., Kome, C., Rolfes, T., Jones, N., Monteith, S. and Matos, M.: Soils and climate of Cul de Sac Valley, Haiti: A soil water and geomorphology perspective. *Journal of Soil and Water Conservation*, *72*(2), pp.91-101. 2017.¶

Deleted: Klose, M., Maurischat, P. and Damm, B.: Landslide impacts in Germany: A historical and socioeconomic perspective. *Landslides*, *13*(1), pp.183-199. 2016.¶

Kritikos, T., Robinson, T.R. and Davies, T.R.: Regional coseismic landslide hazard assessment without historical landslide inventories: A new approach. *Journal of Geophysical Research: Earth Surface*, *120*(4), pp.711-729. 2015.

Lee, E.M. and Jones, D.K.: *Landslide risk assessment*. Thomas Telford. 2004.

Lee, S. and Sambath, T.: Landslide susceptibility mapping in the Damrei Romel area, Cambodia using frequency ratio and logistic regression models. *Environmental Geology*, *50*(6), pp.847-855. 2006.

Lee, S. and Pradhan, B.: Landslide hazard mapping at Selangor, Malaysia using frequency ratio and logistic regression models. *Landslides*, *4*(1), pp.33-41. 2007.

Li, G., West, A.J., Densmore, A.L., Jin, Z., Parker, R.N. and Hilton, R.G.: Seismic mountain building: Landslides associated with the 2008 Wenchuan earthquake in the context of a generalized model for earthquake volume balance. *Geochemistry, Geophysics, Geosystems*, *15*(4), pp.833-844. 2014.

Lin, G.W., Chen, H., Hovius, N., Horng, M.J., Dadson, S., Meunier, P. and Lines, M.: Effects of earthquake and cyclone sequencing on landsliding and fluvial sediment transfer in a mountain catchment. *Earth Surface Processes and Landforms*, *33*(9), pp.1354-1373. 2008.

Marc, O. and Hovius, N., Amalgamation in landslide maps: effects and automatic detection. *Natural Hazards and Earth System Sciences*, *15*(4), pp.723-733. 2015.

McCammon, I.: Heuristic traps in recreational avalanche accidents: Evidence and implications. Avalanche News, 68(1), pp.1-10. 2004.

Mercier de Lépinay, B.M., Deschamps, A., Klingelhoefer, F., Mazabraud, Y., Delouis, B., Clouard, V., Hello, Y., Crozon, J., Marcaillou, B., Graindorge, D. and Vallée, M.: The 2010 Haiti earthquake: A complex fault pattern constrained by seismologic and tectonic observations. *Geophysical Research Letters*, *38*(22). 2011.

Meunier, P., Hovius, N. and Haines, A.J.: Regional patterns of earthquake-triggered landslides and their relation to ground motion. *Geophysical Research Letters*, *34*(20). 2007.

Meunier, P., Hovius, N. and Haines, J.A.: Topographic site effects and the location of earthquake induced landslides. *Earth and Planetary Science Letters*, *275*(3), pp.221-232. 2008.

Formatted: Indent: First line: 0.5 cm

Deleted: Lavé, J. and Avouac, J.P.: Active folding of fluvial terraces across the Siwaliks Hills, Himalayas of central Nepal. *Journal of Geophysical Research: Solid Earth*, *105*(B3), pp.5735-5770. 2000.¶
Lavé, J. and Burbank, D.: Denudation processes and rates in the Transverse Ranges, southern California: Erosional response of a transitional landscape to external and anthropogenic forcing. *Journal of Geophysical Research: Earth Surface*, *109*(F1). 2004.¶

Deleted: Lee, W.H.K., Shin, T.C., Kuo, K.W., Chen, K.C. and Wu, C.F.: CWB free-field strong-motion data from the 21 September Chi-Chi, Taiwan, earthquake. *Bulletin of the seismological society of America*, *91*(5), pp.1370-1376. 2001.¶

Deleted: Li, G., West, A.J., Densmore, A.L., Hammond, D.E., Jin, Z., Zhang, F., Wang, J. and Hilton, R.G.: Connectivity of earthquake-triggered landslides with the fluvial network: Implications for landslide sediment transport after the 2008 Wenchuan earthquake. *Journal of Geophysical Research: Earth Surface*, *121*(4), pp.703-724. 2016.¶
Li, X., Zhou, Z., Yu, H., Wen, R., Lu, D., Huang, M., Zhou, Y. and Cu, J.: Strong motion observations and recordings from the great Wenchuan Earthquake. *Earthquake Engineering and Engineering Vibration*, *7*(3), pp.235-246. 2008.¶

Deleted: Lin, M.L., Wang, K.L. and Chen, T.C.: September. Characteristics of the slope failure caused by Chi-Chi earthquake. In *International workshop on annual commemoration of Chi-Chi earthquake (III): Taipei, National Center for Research on Earthquake Engineering* (pp. 199-209). 2000.¶
Liu-Zeng, J., Wen, L., Oskin, M. and Zeng, L.: Focused modern denudation of the Longmen Shan margin, eastern Tibetan Plateau. *Geochemistry, Geophysics, Geosystems*, *12*(11). 2011.¶
Lupker, M., Blard, P.H., Lave, J., France-Lanord, C., Leanni, L., Puchol, N., Charreau, J. and Bourlès, D.: 10 Be-derived Himalayan denudation rates and sediment budgets in the Ganga basin. *Earth and Planetary Science Letters*, *333*, pp.146-156

Moved down [5]: . 2012.¶

Deleted: MacKinnon, J.R. ed.: *Protected areas systems review of the Indo-Malayan realm*. Asian Bureau for Conservation. 1997.¶

Formatted: Indent: First line: 0.5 cm

Deleted: Meigs, A., Brozovic, N. and Johnson, M.L.: Steady, balanced rates of uplift and erosion of the Santa Monica Mountains, California. *Basin Research*, *11*(1), pp.59-73. 1999.¶

Deleted: Mertens, K., Jacobs, L., Maes, J., Kabaseke, C., Maertens, M., Poesen, J., Kervyn, M. and Vranken, L.: The direct impact of landslides on household income in tropical regions: A case study from the Rwenzori Mountains in Uganda. *Science of the Total Environment*, *550*, pp.1032-1043. 2016.¶

Mills, J.W. and Curtis, A.: Geospatial approaches for disease risk communication in marginalized communities. *Progress in community health partnerships: research, education, and action*, *2*(1), pp.61-72. 2008.

Milledge, D.G., Warburton, J., Lane, S.N. and Stevens, C.J. Testing the influence of topography and material properties on catchment-scale soil moisture patterns using remotely sensed vegetation patterns in a humid temperate catchment, northern Britain. *Hydrological processes*, *27*(8), pp.1223-1237. 2012.

Milledge, D., Rosser, N., Oven, K., Dixit, A.M., Dhungel, R., Basyal, G.K., Adhikari, S.R. and Densmore, A., Simple guidelines to minimise exposure to earthquake-triggered landslides. Earthquake Without Frontiers-Briefing note. 2018. http://eprints.esc.cam.ac.uk/4298/

Montgomery, D.R. and Foufoula-Georgiou, E.: Channel network source representation using digital elevation models. *Water Resources Research*,*29*(12), pp.3925-3934. 1993.

Montgomery, D.R. and Dietrich, W.E.: A physically based model for the topographic control on shallow landsliding. *Water resources research*, *30*(4), pp.1153-1171. 1994.

Moughtin, C.: Barkulti in the Yasmin valley: A study of traditional settlement form as a response to environmental hazard. The International Karakorum Project. Vol. 2, Proceedings of the international conference held at the Royal Geographical Society, London. K. J. Miller. Cambridge: Cambridge University Press: 307-322. 1984.

NCALM: National Centre for Airborne Laser Mapping. *Santa Clarita Topography, Airborne Lidar Data Acquired 06/17/2015*. DOI:10.5069/G9TB14V2. 2015.

Parise, M. and Jibson, R.W.: A seismic landslide susceptibility rating of geologic units based on analysis of characteristics of landslides triggered by the 17 January, 1994 Northridge, California earthquake. *Engineering geology*, *58*(3), pp.251-270. 2000.

Parker, R.N., Rosser, N.J. and Hales, T.C.: Spatial prediction of earthquake-induced landslide probability. *Nat. Hazards Earth Syst. Sci. Discuss., https://doi. org/10.5194/nhess-2017-193, in review*. 2017.

Pradhan, B.: A comparative study on the predictive ability of the decision tree, support vector machine and neuro-fuzzy models in landslide susceptibility mapping using GIS. *Computers & Geosciences*, *51*, pp.350-365. 2013.

Moved (insertion) [5]

Deleted: Montgomery, D.R.: Compressional uplift in the central California Coast Ranges. *Geology*, *21*(6), pp.543-546. 1993.¶

Formatted: Indent: First line: 0.5 cm

Deleted: National Atlas of the United States: *United States Average Annual Precipitation, 1990-2009, Map*, Reston, VA. https://catalog.data.gov/dataset/united-states-average-annual-precipitation-1990-2009-direct-download. 2011.¶
NOAA: Online Weather Data: http://w2.weather.gov/climate/xmacis.php?wfo=sgx. *National Oceanic and Atmospheric Administration*. *Retrieved 2017-10-30. 2017.*¶

Deleted: Olson, D.M., Dinerstein, E., Wikramanayake, E.D., Burgess, N.D., Powell, G.V., Underwood, E.C., D'amico, J.A., Itoua, I., Strand, H.E., Morrison, J.C. and Loucks, C.J.: Terrestrial Ecoregions of the World: A New Map of Life on Earth A new global map of terrestrial ecoregions provides an innovative tool for conserving biodiversity. *BioScience*, *51*(11), pp.933-938. 2001.¶
Ouimet, W.B., Whipple, K.X. and Granger, D.E.: Beyond threshold hillslopes: Channel adjustment to base-level fall in tectonically active mountain ranges. *Geology*, *37*(7), pp.579-582. 2009.¶

Deleted: Paijmans, K., 1975. Explanatory notes to the vegetation map of Papua New Guinea.¶
Peel, M.C., Finlayson, B.L. and McMahon, T.A.: Updated world map of the Köppen-Geiger climate classification. *Hydrology and earth system sciences discussions*, *4*(2), pp.439-473. 2007.¶
Pubellier, M., Mauffret, A., Leroy, S., Vila, J.M. and Amilcar, H.: Plate boundary readjustment in oblique convergence: Example of the Neogene of Hispaniola, Greater Antilles. *Tectonics*, *19*(4), pp.630-648. 2000.¶
Petley, D.: Global patterns of loss of life from landslides. *Geology*,*40*(10), pp.927-930. 2012.¶

Quinn, P., Beven, K., Chevallier, P. and Planchon, O.: The prediction of hillslope flow paths for distributed hydrological modelling using digital terrain models. *Hydrological processes*, *5*(1), pp.59-79. 1991.

Rault, C., Robert, A., Marc, O., Hovius, N. and Meunier, P.: Seismic and geologic controls on spatial clustering of landslides in three large earthquakes. *Earth Surface Dynamics Discussions*. 2018. https://www.earth-surf-dynam-discuss.net/esurf-2018-82/

Roback, K., Clark, M.K., West, A.J., Zekkos, D., Li, G., Gallen, S.F., Chamlagain, D. and Godt, J.W.: The size, distribution, and mobility of landslides caused by the 2015 M w 7.8 Gorkha earthquake, Nepal. *Geomorphology*. 2018.

Roering, J.J., Perron, J.T. and Kirchner, J.W.: Functional relationships between denudation and hillslope form and relief. *Earth and Planetary Science Letters*, *264*(1-2), pp.245-258. 2007.

Schwanghart, W. and Kuhn, N.J.: TopoToolbox: A set of Matlab functions for topographic analysis. *Environmental Modelling & Software*, *25*(6), pp.770-781. 2010.

Shaw, R., Uy, N. and Baumwoll, J.: Indigenous knowledge for disaster risk reduction: Good practices and lessons learned from experiences in the Asia-Pacific Region. *United Nations International Strategy for Disaster Reduction: Bangkok*. 2008.

Shin, T.C. and Teng, T.L.: An overview of the 1999 Chi-Chi, Taiwan, earthquake. *Bulletin of the Seismological Society of America*, *91*(5), pp.895-913. 2001.

Stevens, C., McCaffrey, R., Silver, E.A., Sombo, Z., English, P. and Van der Kevie, J.: Mid-crustal detachment and ramp faulting in the Markham Valley, Papua New Guinea. *Geology*, *26*(9), pp.847-850. 1998.

Stock, J. and Dietrich, W.E.: Valley incision by debris flows: Evidence of a topographic signature. *Water Resources Research*, *39*(4). 2003.

Tanyaş, H., Van Westen, C.J., Allstadt, K.E., Anna Nowicki Jessee, M., Görüm, T., Jibson, R.W., Godt, J.W., Sato, H.P., Schmitt, R.G., Marc, O. and Hovius, N.: Presentation and analysis of a worldwide database of earthquake-induced landslide inventories. *Journal of Geophysical Research: Earth Surface*, *122*(10), pp.1991-2015. 2017.

Taylor, D.W.: *Stability of earth slopes* (pp. 1925-1940). Wright & Potter print. 1937.

Formatted: Indent: First line: 0.5 cm

Deleted: 2017

Deleted: Searle, M.P. and Godin, L.: The South Tibetan detachment and the Manaslu leucogranite: A structural reinterpretation and restoration of the Annapurna-Manaslu Himalaya, Nepal. *The Journal of Geology*, *111*(5), pp.505-523. 2003.¶
Sen, G., Hickey-Vargas, R., Waggoner, D.G. and Maurrasse, F.: Geochemistry of basalts from the Dumisseau Formation, southern Haiti: implications for the origin of the Caribbean Sea crust. *Earth and Planetary Science Letters*, *87*(4), pp.423-437. 1988.¶

Deleted: Singh, J.S. and Singh, S.P.: Forest vegetation of the Himalaya. *The Botanical Review*, *53*(1), pp.80-192. 1987.¶

Formatted: Indent: First line: 0.5 cm

Thompson, M.A., Lindsay, J.M. and Gaillard, J.C.: The influence of probabilistic volcanic hazard map properties on hazard communication.*Journal of Applied Volcanology*, *4*(1), p.1. 2015.

Tibaldi, A., Ferrari, L. and Pasquarè, G.: Landslides triggered by earthquakes and their relations with faults and mountain slope geometry: an example from Ecuador. *Geomorphology*, *11*(3), pp.215-226. 1995.

Travis, M.R., Iverson, W.D., Eisner, G.H. and Johnson, C.G., VIEWIT: computation of seen areas, slope, and aspect for land-use planning. *Gen Tech Rep PSW Pac Southwest For Range Exp Stn USDA For Serv*. 1975.

Twigg, J., Lovell, E., Schofield, H., Miranda Morel, L., Flinn, B., Sargeant, S., Finlayson, A., Dijkstra, T., Stephenson, V., Albuerne, A. and Rossetto, T.: Self-recovery from disasters: an interdisciplinary perspective. *Overseas Development Institute: London, UK*. 2017.

Deleted: Tsutsumi, H. and Yeats, R.S.: Tectonic setting of the 1971 Sylmar and 1994 Northridge earthquakes in the San Fernando Valley, California. *Bulletin of the Seismological Society of America*, *89*(5), pp.1232-1249. 1999. ¶

Volkwein, A., Schellenberg, K., Labiouse, V., Agliardi, F., Berger, F., Bourrier, F., Dorren, L.K., Gerber, W. and Jaboyedoff, M.: Rockfall characterisation and structural protection-a review. *Natural Hazards and Earth System Sciences*, *11*, pp.p-2617. 2011.

von Ruette, J., Lehmann, P. and Or, D. Linking rainfall-induced landslides with predictions of debris flow runout distances. *Landslides*, *13*(5), pp.1097-1107. 2016.

Wald, D.J. and Heaton, T.H.: *A dislocation model of the 1994 Northridge, California, earthquake determined from strong ground motions* (No. 94-278). US Geological Survey. 1994.

Wang, W.N., Wu, H.L., Nakamura, H., Wu, S.C., Ouyang, S. and Yu, M.F.: Mass movements caused by recent tectonic activity: the 1999 Chi-chi earthquake in central Taiwan. *Island Arc*, *12*(4), pp.325-334. 2003.

Williams, J.G., Rosser, N.J., Kincey, M.E., Benjamin, J., Oven, K.J., Densmore, A.L., Milledge, D.G., Robinson, T.R., Jordan, C.A. and Dijkstra, T.A.: Satellite-based emergency mapping using optical imagery: experience and reflections from the 2015 Nepal earthquakes. *Natural hazards and earth system sciences.*, *18*, pp.185-205. 2018.

Moved (insertion) [4]

Deleted: Xu, C.,

Formatted: English (United States)

Xu, C., Xu, X., Dai, F. and Saraf, A.K.: Comparison of different models for susceptibility mapping of earthquake triggered landslides related with the 2008 Wenchuan earthquake in China. *Computers & Geosciences*, *46*, pp.317-329. 2012.

Formatted: Indent: First line: 0.5 cm

Moved (insertion) [6]

Xu, C., Shyu, J.B.H. and Xu, X.: Landslides triggered by the 12 January 2010 Port-au-Prince, Haiti, Mw= 7.0 earthquake: visual interpretation, inventory compiling, and spatial distribution statistical analysis. *Natural Hazards and Earth System Sciences*, *14*(7), p.1789. 2014.

Xu, C., Xu, X., Yao, X. and Dai, F.: Three (nearly) complete inventories of landslides triggered by the May 12, 2008 Wenchuan Mw 7.9 earthquake of China and their spatial distribution statistical analysis. *Landslides*, *11*(3), pp.441-461. 2014.

Yilmaz, I.: Landslide susceptibility mapping using frequency ratio, logistic regression, artificial neural networks and their comparison: a case study from Kat landslides (Tokat—Turkey). *Computers & Geosciences*, *35*(6), pp.1125-1138. 2009.

Yin, K.L. and Yan, T.Z.: July. Statistical prediction model for slope instability of metamorphosed rocks. In *Proceedings of the 5th international symposium on landslides, Lausanne, Switzerland* (Vol. 2, pp. 1269-1272). AA Balkema Rotterdam, The Netherlands. 1988.

Moved up [6]: Dai, F. and Saraf, A.K.: Comparison of different models for susceptibility mapping of earthquake triggered landslides related with the 2008 Wenchuan earthquake in China. *Computers & Geosciences*, *46*, pp.317-329. 2012.¶
Xu, C.,

Formatted: Indent: First line: 0.5 cm

Deleted: Xu, X. and Yu, G.: Landslides triggered by slipping-fault-generated earthquake on a plateau: an example of the 14 April 2010, Ms 7.1, Yushu, China earthquake. *Landslides*, *10*(4), pp.421-431. 2013.¶
Xu, X., Wen, X., Yu, G., Chen, G., Klinger, Y., Hubbard, J. and Shaw, J.: Coseismic reverse-and oblique-slip surface faulting generated by the 2008 Mw 7.9 Wenchuan earthquake, China. *Geology*, *37*(6), pp.515-518. 2009.¶
Wu, C.C. and Kuo, Y.H.: Typhoons affecting Taiwan: Current understanding and future challenges. *Bulletin of the American Meteorological Society*, *80*(1), pp.67-80. 1999.¶

Deleted: ¶
Yu, G., Tang, L., Yang, X., Ke, X. and Harrison, S.P.: Modern pollen samples from alpine vegetation on the Tibetan Plateau. *Global Ecology and Biogeography*, *10*(5), pp.503-519. 2001.